Trajectory hunting as an effective technique to validate multiplatform measurements: Analysis of the MLS, HALOE, SAGE-II, ILAS, and POAM-II data in October–November 1996

M. Y. Danilin,[1] M. K. W. Ko,[2] L. Froidevaux,[3] M. L. Santee,[3] L. V. Lyjak,[4] R. M. Bevilacqua,[5] J. M. Zawodny,[6] Y. Sasano,[7] H. Irie,[8] Y. Kondo,[8] J. M. Russell III,[9] C. J. Scott,[2] and W. G. Read[3]

Received 17 December 2001; revised 19 April 2002; accepted 17 June 2002; published 19 October 2002.

[1] The goal of this study is to show that trajectory hunting is an effective technique for comparison of multiplatform measurements. In order to achieve this goal, we (1) describe in detail the trajectory hunting technique (THT), (2) perform several consistency tests for THT (self-hunting and reversibility), (3) estimate uncertainties of this technique, and (4) validate THT results against those obtained by the traditional correlative analysis (TCA). THT launches backward and forward trajectories from the locations of measurements and finds air parcels sampled at least twice within a prescribed match criterion during the course of several days. TCA finds matched profiles for a chosen match criterion, averages them for each instrument separately, and compares the averaged profiles. As an example, we consider the 22 October to 30 November 1996 period in the Southern Hemisphere and compare the latest versions of relevant measurements made by the following five instruments: Microwave Limb Sounder (MLS, version 5 (v.5)), Halogen Occultation Experiment (HALOE, v.19), Polar Ozone and Aerosol Measurement II (POAM-II, v.6), Stratospheric Aerosol and Gas Experiment II (SAGE-II, v.6.1), and Improved Limb Atmospheric Spectrometer (ILAS, v.5.20). We present results for O_3, H_2O, CH_4, HNO_3, and NO_2, which show that (1) ozone measurements from all five instruments agree to better than 0.4 (0.2) ppmv below (above) 30 km; (2) water vapor measurements agree within ±5–10% above 22 km; (3) methane measurements by HALOE and ILAS agree to better than 10% above 30 km with a possible positive offset of up to 10–15% by ILAS in the lower stratosphere; (4) MLS HNO_3 data corrected to account for some excited vibrational lines omitted in the v.5 HNO_3 retrieval agree with ILAS HNO_3 measurements to within ~0.5 ppbv (~10–20%) over the range ~450–750 K; (5) ILAS sunset NO_2 measurements are larger than both POAM-II and SAGE-II values by up to 10–15% below 30 km. The self-hunting tests show that the THT RMS noise is of the order of 1–2% for O_3, CH_4, and H_2O and 4% for NO_2 and HNO_3 measurements in the stratosphere. Total THT-related uncertainties may be 3–5% for O_3 measurements when photochemical effects and sensitivities of the results to duration of trajectories and match criteria are taken into account. Good agreement is found between the THT and TCA results for each of these products and for each possible pair of instruments, with considerably better statistics (typically by at least an order of magnitude) in the THT case. This agreement validates the THT results. *INDEX TERMS:* 0341 Atmospheric Composition and Structure: Middle atmosphere—constituent transport and chemistry (3334); 0394 Atmospheric Composition and Structure: Instruments and techniques; 0340 Atmospheric Composition and Structure: Middle atmosphere—composition and chemistry; *KEYWORDS:* trajectory hunting, satellite measurements, validation technique

Citation: Danilin, M. Y., et al., Trajectory hunting as an effective technique to validate multiplatform measurements: Analysis of the MLS, HALOE, SAGE-II, ILAS, and POAM-II data in October–November 1996, *J. Geophys. Res.*, *107*(D20), 4420, doi:10.1029/2001JD002012, 2002.

[1]The Boeing Company, Seattle, Washington, USA.
[2]Atmospheric and Environmental Research, Inc., Lexington, Massachusetts, USA.
[3]Jet Propulsion Laboratory, Pasadena, California, USA.
[4]National Center for Atmospheric Research, Boulder, Colorado, USA.
[5]Naval Research Laboratory, Washington, District of Columbia, USA.
[6]NASA Langley Research Center, Hampton, Virginia, USA.
[7]NIES, Tsukuba, Ibaraki, Japan.
[8]University of Tokyo, Tokyo, Japan.
[9]Hampton University, Hampton, Virginia, USA.

0148-0227/02/2001JD002012$09.00

1. Introduction

[2] Any new instrument must be properly calibrated and validated before its products can be used for scientific studies. A conventional way to validate a new instrument (traditional correlative analysis, TCA) is to compare its measurements to similar data obtained by other well-established platforms which are colocated as closely as possible in time and space. Typically, data sets of two instruments of interest, overlapping in time and space, are browsed in order to find colocated profiles which satisfy a given match criterion. Then the mean profiles of each instrument are found by averaging all matched profiles for each instrument and the difference (in percent or in absolute units) between them is analyzed for a possible bias of one instrument versus another (see the following special issues of *Journal of Geophysical Research: 94*(D6), 1989; *101*(D6), 9539–10,476, 1996; *102*(D19), 1997, devoted to validation of the Stratospheric Aerosol and Gas Experiment II (SAGE-II), Upper Atmosphere Research Satellite (UARS), and Polar Ozone and Aerosol Measurement II (POAM-II), respectively). However, a relatively small amount of matches (particularly for the occultation instruments with only 28–30 profiles per day [e.g., *Lu et al.*, 1997, 2000]) can limit the statistical significance of new satellite platform validation. In order to better detect possible biases in measurements by a new instrument, it makes sense to perform a comparison with several other instruments. In order to accomplish this goal, one should make sure that the same air masses are compared. Equivalence of the air masses is clearly seen in potential temperature-equivalent latitude coordinates, which remove the meteorological variability [e.g., *Schoeberl et al.*, 1995; *Manney et al.*, 1999]. Recently, *Manney et al.* [2001] compared ozone measurements made by seven different satellite instruments in November 1994 using potential temperature-equivalent latitude coordinates and found that they agreed usually within 0.5 (0.25) ppmv in the upper (lower) stratosphere. Several Lagrangian techniques have been applied to improve the comparison of satellite data with model calculations or in situ measurements. *Pierce et al.* [1994] created "synoptic" maps of Halogen Occultation Experiment (HALOE) measurements for improving the statistical significance of its sunrise and sunset measurement comparison. *Sutton et al.* [1994] used the reverse-domain-filling technique in order to create uniformly gridded satellite data by initializing trajectories on a regular grid and then assigning them values of the satellite measurements according to their encounters with backward trajectories. *Von der Gathen* [1995] and *Rex et al.* [1998] applied the so-called Match technique to find air parcels sampled twice by ozonesondes in the Arctic lower stratosphere and to calculate ozone loss rates for the matched parcels there. The above studies did not use a photochemical box model to accomplish their goals. *Austin et al.* [1987] demonstrated the power of the Lagrangian approach in using Limb Infrared Monitor of the Stratosphere (LIMS) data to test photochemical mechanisms by finding matched air parcels and comparing model calculations of O_3, NO_2, and HNO_3 against their LIMS measurements along these trajectories. *Pierce et al.* [1997] applied photochemical calculations along trajectories to compare ER-2 and HALOE measurements and model calculations of the radical species against ER-2 measurements. *Becker et al.* [1998] applied photochemical calculations along the matched air trajectories to compare observed and calculated ozone loss rates in the Arctic during the 1991/92 winter. *Danilin et al.* [2000] used the AER box model with different PSC schemes along air parcels sampled at least twice by UARS during a 5-day period in December 1992. They obtained a reasonable agreement between calculated and measured behavior of ClO, $ClONO_2$, HNO_3, and aerosol extinction at 780 cm^{-1} during this episode. Recently, *Danilin et al.* [2002] compared the ER-2 and satellite measurements of O_3, H_2O, ClO, and HNO_3 during the SOLVE campaign, using the AER box model constrained by the relevant ER-2 measurements.

[3] This study is aimed at quantifying the uncertainties of the trajectory hunting technique (THT) and comparing the THT results against those obtained by the TCA, so as to demonstrate how a comparison of multiplatform measurements may be improved by applying the THT. The term "trajectory hunting" outlines the fact that not all trajectories launched from the locations of observations of interest are used in a further analysis, but only those which found matches (or were successfully hunted) among other platform measurements. We believe that the THT facilitates systematic validation studies of the multiplatform measurements and is particularly attractive for rapid validation of new instruments shortly after their deployment because of the large number of matches provided by THT.

[4] THT is conceptually similar to the Match technique [*Rex et al.*, 1998]. However, the match technique has been applied so far only to deriving ozone loss rates using the matched ozonesonde measurements. A trajectory mapping technique [*Morris et al.*, 1995] has been used to create synoptic-scale maps of different instrument measurements for their subsequent comparison (e.g., HALOE and Microwave Limb Sounder (MLS) H_2O). Later, *Morris et al.* [2000] showed that trajectory mapping is an effective tool in validation of different satellite measurements and in estimating instrument precision (using MLS H_2O measurements as an example). In order to validate measurements made by two instruments, *Morris et al.* [2000] created a synoptic map from the data set with better coverage (e.g., MLS) at the time of each measurement by the second instrument (e.g., HALOE). A similar approach was used by *Bacmeister et al.* [1999] for comparison of the ER-2 and CRISTA measurements of O_3, CFC-11, and NO_y by advecting the 2 and 4 November 1994, ER-2 flights and CRISTA data to a noon time on 5 November 1994. So far, there has not been a comparison of the results obtained by the trajectory mapping and trajectory hunting. It is quite possible that these two techniques may provide similar results. However, we believe that THT has the following three advantages: (1) less computational efforts are required, since we do not advect dense measurements (like MLS or CLAES), (2) THT does not perform horizontal interpolation in order to compare two synoptic maps of the two sets of measurements, and (3) our results are not sensitive to a choice of a particular time, for which trajectory mapping is performed.

[5] On the other hand, there are several caveats associated with the THT. First, this technique should not be directly used for a species with a short photochemical lifetime or experiencing rapid microphysical changes (like

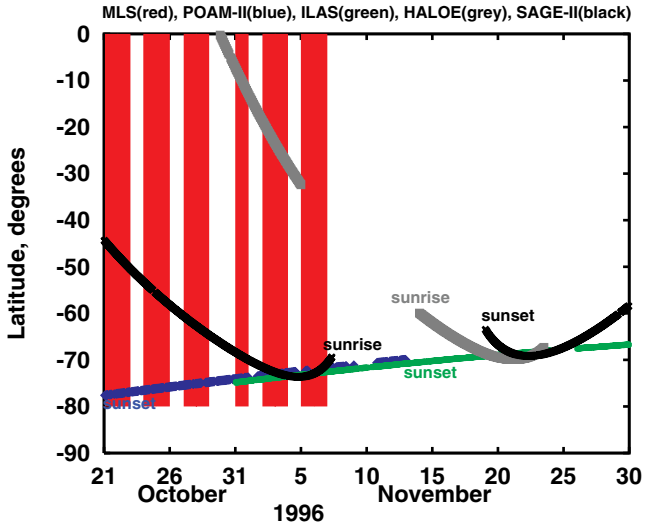

Figure 1. Latitudinal coverage of the MLS (red), HALOE (grey), SAGE-II (black), POAM-II (blue), and ILAS (green) measurements in the southern hemisphere during the 21 October–30 November 1996 period.

condensation or evaporation of H_2O and HNO_3 from polar stratospheric clouds). A photochemical or microphysical model is required in these cases. Second, the obtained THT results are linked to a particular meteorological situation and data set chosen and may not be considered as general results. Third, trajectory calculations and possible model analysis for the matched air parcels introduce their own uncertainties which should be properly taken into account.

[6] The structure of our paper is the following. Section 2 characterizes the period chosen for our analysis and considers the main features of the instruments used. Sections 3 describes in detail the THT. In section 4 we demonstrate the self-consistency and validity of the THT using several different examples. The following five sections provide results of the ozone, water vapor, methane, nitric acid, and nitrogen dioxide measurement comparison, respectively. Finally, the last section summarizes the main findings of our study and provides an outlook for possible future research.

2. Period Considered and Instruments Used

[7] Figure 1 shows latitude coverage by the MLS (red), POAM-II (blue), SAGE-II (black), HALOE (grey), and Improved Limb Atmospheric Spectrometer (ILAS) (green) instruments from 22 October to 30 November 1996. The following reasons determine our choice of this time period. First, these five instruments sampled the atmosphere in a relatively narrow latitudinal band of 70°–80°S during the 40-day period shown in Figure 1. Such a compact sampling of near-coincident air masses should provide many matches for validation of these multiplatform measurements. Second, numerous matches obtained by TCA during this episode may serve for validation of the trajectory hunting technique. Third, this time period allows us to compare different measurement techniques (for example, MLS is a limb emission instrument measuring at any local solar zenith angle, while the rest use the occultation technique measuring only at local sunrise or sunset).

[8] During the period shown, POAM-II stopped operation on 14 November because of the failure of the host SPOT-III satellite. On the other hand, ILAS started to provide about 14 sunset profiles daily in the Southern Hemisphere on a regular basis after November 1. The ILAS and POAM-II sampling geometry is very similar, providing near-coincident data from 1 to 13 November. MLS made its last south-looking (i.e., from 80°S to 34°N) measurements on 7 November 1996, before a yaw maneuver changed its latitudinal coverage to 34°S to 80°N. Also, there were gaps in the MLS data on 24 and 27 October, 30 October to 1 November, and 5 November 1996. HALOE sunrise measurements in the Southern Hemisphere were available from 30 October to 24 November, with a gap from 6 to 14 November caused by a HALOE power-off. The SAGE-II measurements in the Southern Hemisphere were available until 8 November (sunrise) and after 20 November (sunset). The occultation instrument sunset and sunrise measurements correspond to the local sunset and sunrise conditions, respectively, during the period considered.

[9] Table 1 summarizes the instruments, their principal references and parameters used in this study. The period

Table 1. Instruments, Their Web Sites, Principal References[a], and Characteristics[b]

Instrument	Web Site	Species Measured[c]	Version	Δz, km	Profiles per Day
MLS	mls.jpl.nasa.gov	O_3, HNO_3	5	4–6[d]	~1300
POAM-II	wvms.nrl.navy.mil/POAM	O_3, NO_2	6	1	28
ILAS	www-ilas.nies.go.jp	O_3, NO_2, HNO_3, H_2O, CH_4	5.20	~2	28
HALOE	haloedata.larc.nasa.gov	O_3, NO_2, H_2O, CH_4	19	2	30
SAGE-II	www-sage2.larc.nasa.gov	O_3, NO_2, H_2O	6.1	0.75–1.25[e]	28

[a] Instrument descriptions: MLS [*Waters*, 1993; *Barath et al.*, 1993], POAM-II [*Glaccum et al.*, 1996; *Bevilacqua*, 1997], HALOE [*Russell et al.*, 1993], ILAS [*Sasano et al.*, 1999a; *Suzuki et al.*, 1995], SAGE-II [*Russell and McCormick*, 1993]; Validation papers: MLS O_3 v.3 [*Froidevaux et al.*, 1996] and v.5 (Livesey et al., submitted manuscript, 2002); MLS HNO_3 v.4 [*Santee et al.*, 1999, 2000] and v.5 (Livesey et al., submitted manuscript, 2002); POAM-II O_3 v.5 [*Rusch et al.*, 1997; *Deniel et al.*, 1997] and NO_2 [*Randall et al.*, 1998]; ILAS v.3.10 O_3 [*Sasano et al.*, 1999b] and v.5.20 O_3 [*Sugita et al.*, 2002], ILAS v.5.20 H_2O [*Kanzawa et al.*, 2002], CH_4 [*Toon et al.*, 2002; *Kanzawa et al.*, 2002], HNO_3 [*Irie et al.*, 2002], and NO_2 [*Irie et al.*, 2002]; HALOE v.17 O_3 [*Brühl et al.*, 1996], H_2O [*Harries et al.*, 1996], CH_4 [*Park et al.*, 1996], and NO_2 [*Gordley et al.*, 1996]; SAGE-II v.6.0 O_3 [*Manney et al.*, 2001], v.5.93 H_2O [*Chu et al.*, 1993], and v.5.9 NO_2 [*Cunnold et al.*, 1991].

[b] Parameters shown are measured species, version used, approximate vertical resolution Δz, and profiles per day.

[c] Only species compared in this study are shown.

[d] 4 km for O_3 and 6 km for HNO_3.

[e] 0.75 km for O_3 and 1.5 km for NO_2 and H_2O.

considered also allows a comparison of aerosol extinction measurements made by ILAS, POAM-II, SAGE-II, and HALOE. Such a comparison can be made easily for extinctions measured at the same wavelengths (e.g., at 780 nm by POAM-II and ILAS). However, it requires additional considerable effort to compare aerosol extinction measurements made at different wavelengths. We decided that a thorough analysis of these four instruments' aerosol data should be a subject for a separate study.

3. Trajectory Hunting Technique

[10] According to our definition, trajectory hunting is a technique to find air parcels sampled at least twice by the same or different platforms over the course of a few days [*Danilin et al.*, 2000]. There are four stages in applying the THT for validation studies.

[11] In the first stage, backward and forward diabatic trajectories are calculated for each point of the measurements considered. We used 5-day trajectories. However, the length of the trajectories is arbitrary. One should keep in mind that longer trajectories, especially under the meteorological conditions in this study, potentially may accumulate larger uncertainties in calculations of their locations [e.g., *Austin*, 1986; *Schoeberl and Sparling*, 1994; *Morris et al.*, 1995]. Also, photochemical processes and mixing limit usefulness of longer trajectories. Platforms whose measurements were origination points of the trajectories are called "hunters." Platforms whose profiles are targeted by the trajectories are called "targets." From a practical standpoint (i.e., less computer resources are required), it is better to launch trajectories from the locations of the relatively sparse measurements (like HALOE) and to hunt in more dense clouds of measurements (like MLS) rather than vice versa. In this study we used 339, 106, 420, and 367 profiles of ILAS, POAM-II, SAGE-II, and HALOE, respectively, for the trajectory calculations during the period shown in Figure 1. We launched backward and forward trajectories with a vertical step of 1 km from 15 to 50 km for the ILAS and HALOE locations, from 10 to 45 km for the SAGE-II locations, and from 15 to 40 km for the POAM-II locations. Thus, the total number of trajectories calculated in each direction (i.e., backward and forward) was 12,204, 13,212, 15,120, and 2756 for the ILAS, HALOE, SAGE-II, and POAM-II locations, respectively. No trajectories were calculated from the MLS locations because of the high frequency of the MLS measurements, requiring a large amount of computer memory. We did not calculate trajectories below 15 km because some instruments (MLS) do not provide reliable measurements below this level or some products (like POAM-II NO_2) are missing. Above 50 km trajectories are not calculated because (1) some species have a short photochemical lifetime and (2) mixing with ambient air becomes rapid [*Shepherd et al.*, 2000], thus limiting the effectiveness of the THT there. However, mixing with ambient air in the lower and middle stratosphere is quite slow (with a typical timescale of several tens of days [*Prather and Jaffe*, 1990]), thus it does not affect noticeably our THT results, which are separated on average by 2–3 days.

[12] The diabatic trajectories used in this study were computed using a fourth-order Runge-Kutta method with adaptive step control [*Press et al.*, 1986]. A further refinement of the algorithm was to repeatedly calculate each trajectory, doubling the integration routine's accuracy with each new integration until successive trajectories differed from each other by an average horizontal distance of less than 100 km. Temperature and geopotential height fields from the U.K. Meteorological Office assimilation scheme [*Swinbank and O'Neill*, 1994] were used to calculate the once-daily three-dimensional wind field. We use these fields instead of the UKMO-derived wind fields for the following reasons: (1) our trajectory code is used with different meteorological data sets, some of which do not have wind fields, and (2) we want to calculate vertical velocities in a self-consistent way, since there is some concern about UKMO-produced vertical velocities [*Massie et al.*, 2000]. Our comparisons (not shown here) depict a very small difference between our and UKMO horizontal wind fields. These data are on a global latitude-longitude grid of 2.5° by 3.75° and on a vertical grid of the UARS levels (i.e., six levels per decade of pressure) between 1000 and 0.32 hPa. The zonal mean wind is calculated using the gradient zonal wind approximation. The eddy components of the zonal and meridional winds are obtained using an approximation that is consistent with the zonal mean gradient zonal wind. The mean meridional wind and the vertical wind (mean and eddy components) were calculated using the thermodynamic and continuity equations in the same manner as shown by *Smith and Lyjak* [1985]. The net diabatic heating rates used in the thermodynamic equation were calculated as described by *Gille and Lyjak* [1986] using the UKMO temperatures and monthly mean H_2O and O_3 climatologies. We use diabatic trajectories here, since they should better represent the vertical motions in the atmosphere compared with that in adiabatic trajectories. However, the difference between them is perhaps small since the mean temporal distance between matches is 2–3 days. The three-dimensional wind at the locations and times required by the trajectory calculation was obtained by linearly interpolating in space and time. Potential vorticity was also calculated from these winds. Our trajectory code is a commonly accepted source of trajectory calculations and shows a good agreement (not shown here) with the results of the Goddard Automailer [*Schoeberl and Sparling*, 1994] and the NOAA Hybrid Single-Particle Lagrangian Integrated Trajectory 4 (HYPSLIT4) model (visit www.arl.noaa.gov/ready/hypsli4.html for details).

[13] At the second stage of the THT, after launching trajectories from the point of interest, we check whether these air parcels pass within a prescribed temporal-spatial distance from the targeted measurements. If so, the hunting for this trajectory is successful and it is a subject for further analysis; if not, we drop this trajectory from any further consideration. We describe the time and location of each measurement in terms of its partial Julian day, latitude, longitude, and potential temperature. It is reasonable to anticipate more matches for more relaxed match criteria, more dense measurements and longer trajectories. Our sensitivity studies in the next section will confirm this statement.

[14] The third stage is devoted to establishing a correspondence between the same products measured by different instruments at the matched points, or pairing measured

values. The values of the species of interest at the origination points of the trajectories are known. The corresponding value of the same species measured by the targeted instrument is found by interpolation in the vertical coordinate of the matched profile. For example, if a SAGE-II trajectory hits an MLS profile at 50 hPa, a corresponding MLS ozone value is defined by a linear interpolation in a log(pressure) coordinate of the MLS O_3 values at 46 and 68 hPa. Our sensitivity analysis shows that the choice of vertical coordinate (e.g., potential temperature versus pressure) does not affect the results noticeably. The number of matched points can be different for the various species, since their vertical coverage differs. For example, POAM-II does not report NO_2 concentration below 20 km, while the ozone profile below 20 km is provided. Thus, the total number of matched points for the POAM-II ozone data may be larger than that for the POAM II NO_2 measurements.

[15] At the final, fourth stage, grouping and statistical analysis of the matched measurements are performed. We call "grouping" a procedure that bins all matched data as a function of vertical coordinate (like potential temperature, pressure or altitude). Below we use potential temperature as a natural coordinate for the THT and bin all matched measurements with a 50 K step below 1000 K (~34 km) and with a 100 K step above 1000 K.

[16] The error bars in the figures represent the standard error of the mean differences (±1σ or 68% confidence level) and are determined according to:

$$ERR = SD/\sqrt{N}, \tag{1}$$

here N is the number of matches at a particular vertical bin and SD is the standard deviation of the differences and is defined according to:

$$SD = \sqrt{\sum_{i=1}^{N} \left(\Delta_i - \bar{\Delta}\right)^2/(N-1)} \tag{2}$$

here $\bar{\Delta} = \Sigma_{i=1}^{N} \Delta_i/\mathrm{N}$ is the mean difference between the two instrument measurements and Δ_i is the difference for the ith pair (e.g., $\Delta_i = O_{3i}^{MLS} - O_{3i}^{POAM\text{-}II}$). The values of Δ_i can be expressed either in absolute (ppmv or ppbv) or relative (%) units. The standard deviation characterizes the spread of the distribution near the mean value (i.e., $\bar{\Delta}$) and is a measure of the combined random error of both instruments. Thus, it does not account for the systematic errors.

[17] This description of the THT shows that TCA is a partial case of the THT, when a required match is obtained near initial points of the trajectories. Thus, the THT should provide more matches than TCA for validation of atmospheric measurements. Figure 2 illustrates this point by comparing the number of matches obtained by the TCA (top panel) and THT (bottom panel). For the match criterion of (Δtime $\leq$ 2 h, Δlatitude $\leq$ 2°, Δlongitude $\leq$ 2°) (or simply (2 h, 2°, 2°)), we found zero matches using TCA on 1 November 1996 during a 2-hour interval between 0500 and 0700 UT. However, launching backward (cyan line) and forward (black line) trajectories from the ILAS location (a green dot at 74.7°S, 113.3°W) at 548 K (~22 km), we found 19 matches (16, 2, and 1 matches with MLS (red dots), POAM-II (blue dots), and SAGE-II (black dot) measurements, respectively). While the number of matches using THT varies at different levels and different

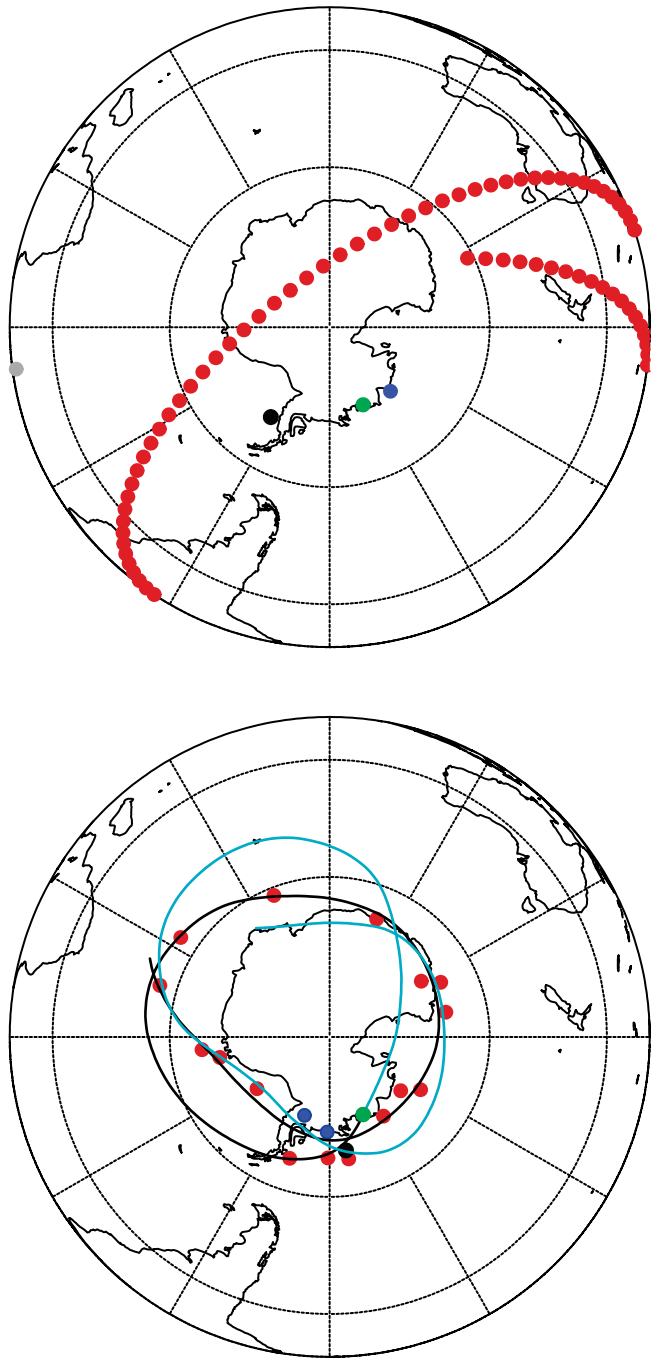

Figure 2. (top panel) Zero matches are found using TCA on 1 November 1996 during a 2-h interval from 5 to 7 h GMT with a match criterion of (2 h, 2°, 2°) for the MLS (red dots), ILAS (green dot), POAM-II (blue dot), SAGE-II (black dot), and HALOE (grey dot). (bottom panel) Applying THT and launching 5-day backward (cyan line) and forward (black line) trajectories at 548 ~ K from the ILAS point at 74.7°S, 113.3°W (shown by a green dot), we found 16, 2, and 1 matches with the MLS, POAM-II, and SAGE-II, respectively, for the same match criterion.

days, the general pattern remains the same, confirming that the THT provides many more matches than the TCA. Below we quantify the advantages and the limitations of the THT.

4. Testing Consistency of THT

4.1. Self-Hunting

[18] Before applying THT for comparing different platform measurements, it makes sense to check this technique for analysis of the same instrument data. During this procedure, trajectories are launched from the ILAS, SAGE-II, HALOE, and POAM-II points and only the same platform measurements are targeted. We call this test "self-hunting." The self-hunting provides (1) an additional test for the precision of the instrument products studied and (2) estimates of the quality of the trajectory calculated, thus assessing the noise of the THT. One may anticipate zero changes at all altitudes if the product measured is a passive tracer and the THT results are noise-free. Additionally, the number of matches for the backward and forward trajectories should be almost equal, since the matched points should be linked by both forward and backward trajectories and each forward trajectory has its own backward analog during the self-hunting.

[19] Figure 3 shows the self-hunting results for ozone, water vapor, nitrogen dioxide, methane, and nitric acid. In general, the difference curves oscillate near the zero vertical line for each product and each instrument, illustrating the robustness of the THT. The error bars, usually overlapping the zero vertical lines, show that the obtained differences may be explained by random noise. The main exception are the result for HNO_3 (panel e) above ~40 km, where deviations of up to 20% were observed. The reasons for this are (1) the short photochemical lifetime of nitric acid (several hours against photolysis in the upper stratosphere), which invalidates the assumption that HNO_3 can be treated as a passive tracer, and (2) the low absolute values of HNO_3 (less than 1 ppbv), which produce large relative errors even for small absolute differences. Surprisingly stable results for short-lived NO_2 are caused by the fact that the matched measurements were made at the same solar zenith angle (at sunset for POAM-II and ILAS and at sunrise for HALOE), thus negating the strong diurnal variability of NO_2. Since the mean temperature change between the matched points was relatively small (several degrees Kelvin), total NO_y was conserved (since no denitrification occurred along the matched trajectories because of the warm temperature) and ozone changes were small (see the next section). Thus, it is reasonable to assume that NO_2 was in a steady state [*Kawa et al.*, 1993], allowing a direct comparison of the NO_2 values at the matched points. Water vapor definitely can be considered as a passive tracer, since (1) its photochemical lifetime is much longer than several days below 50 km and (2) temperature along the matched trajectories was always above the ice frost point, thus precluding H_2O condensation in the ice particles. Methane is also a long-lived species in the stratosphere, with a photochemical lifetime longer than a year; thus it can be treated as an inert tracer. Ozone in the lower stratosphere also can be treated as a passive tracer. However, above 40 km its photochemical lifetime becomes shorter and comparable to 2–3 days (i.e., the mean interval between the matches). For this reason, the results shown in Figure 3a are less trustworthy near 45–50 km and their vicinity to zero may be explained by a possible compensation of the photochemical changes along a similar portion of the backward and forward trajectories.

[20] The main conclusion of this figure is an estimate of the THT noise, which can be defined as the root-mean square (rms) difference for each instrument and altitudes shown in Figure 3. Following this definition, we conclude that the THT does not allow determination of a bias of one instrument against another to better than 1–2% for O_3, H_2O, and CH_4 and 4% for NO_2 and HNO_3. These values are the THT "noise" for these products in the stratosphere.

[21] For perfectly calculated trajectories, the number of matches for the forward and backward trajectories for the self-hunting case should be almost equal. Thus, differences between these two numbers characterize the quality of the trajectory calculations. Since the numbers of matches for the forward and backward trajectories are close to each other (within 1–2%), we conclude that the trajectories are calculated in a self-consistent way.

[22] Summarizing, the results in Figure 3 show that the THT passes the first consistency test and provides estimates of the noise of this technique. However, the results obtained here are valid for the period considered and may vary for different seasons and locations.

4.2. Reversibility

[23] Another important consistency test of the THT is the sensitivity of the THT results to the choice of hunter (i.e., measurement locations from which trajectories are originated) and target (i.e., measurement locations which are targeted by the trajectories). Obviously, the THT results should be insensitive to this choice. Fundamental differences in the retrieval algorithms (e.g., spectroscopic data used, numerical solutions of the radiative transfer equations, assumptions made for their solution, etc.) may cause biases between instruments. These biases should not be sensitive to the way the trajectory hunting was performed (i.e., launching trajectories from the locations of instrument A profiles and hunting against instrument B profiles or vice versa). In order to test this, we perform trajectory hunting for an ILAS/SAGE-II pair of O_3 measurements, launching trajectories from both instruments. Figure 4 shows the results of this test. The main feature we want to underline is the almost identical behavior of the two curves shown in Figure 4. The slight difference in the total number of matches (4458 versus 4847) and number of matches at each level shown in Figure 4 for the ILAS→SAGE-II and SAGE-II→ILAS hunting can be explain by the fact that 12,564 SAGE-II trajectories were launched hunting for 339 ILAS profiles, while 12,204 ILAS trajectories hunted for 349 SAGE-II profiles.

[24] We also performed additional reversibility tests for the ILAS/POAM-II O_3 measurements and again obtained very good agreement between POAM-II→ILAS and ILAS→POAM-II results (not shown here). This reversibility test confirms the insensitivity of the THT results to the choice of hunter and target. Therefore, for each measurement pair evaluated in this study, we perform the calcula-

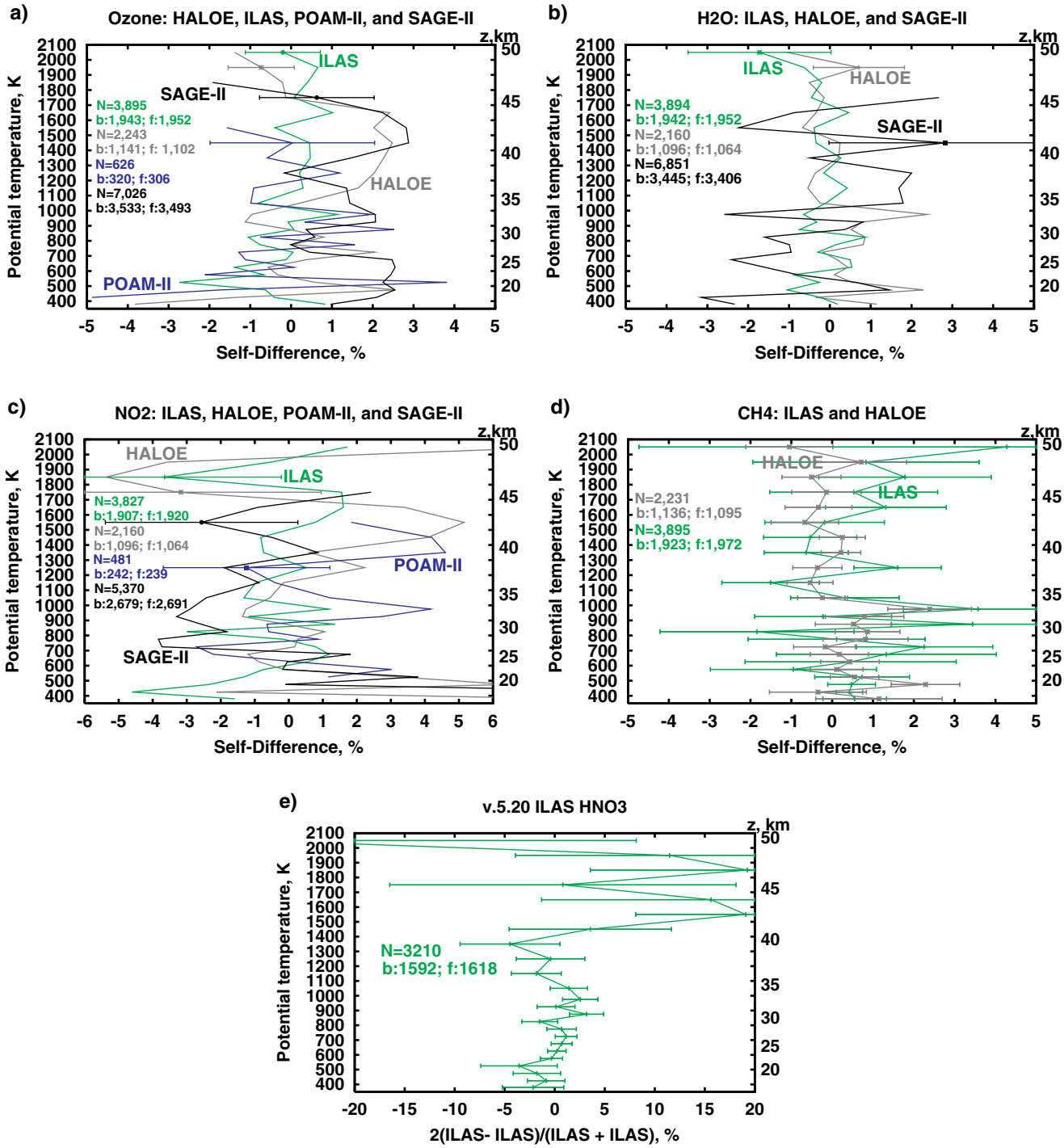

Figure 3. Self-hunting results for the ILAS (green), HALOE (grey), POAM-II (blue), and SAGE-II (black) measurements of ozone (panel a), water vapor (panel b), nitrogen dioxide (panel c), methane (panel d), and nitric acid (panel e). Total numbers of matches N (including their partitioning between backward and forward trajectories, marked as b: and f:, respectively) are color coded according to Figure 1 for each product. MLS measurements are not shown because of the lack of trajectories originating from their locations.

tions for only one choice of hunter and target rather than doing two sets of calculations for each measurement pair.

4.3. Estimating Effects of Photochemistry

[25] Since the ozone photochemical lifetime becomes short (i.e., several days or shorter) above 35–40 km under sunlit conditions and comparable to the mean temporal distance between matches of about 2 days (see Table 2), it is important to estimate the effect of photochemical changes on the ozone results. The obvious approach is to apply a photochemical box model constrained by available satellite measurements in order to estimate photochemical changes in

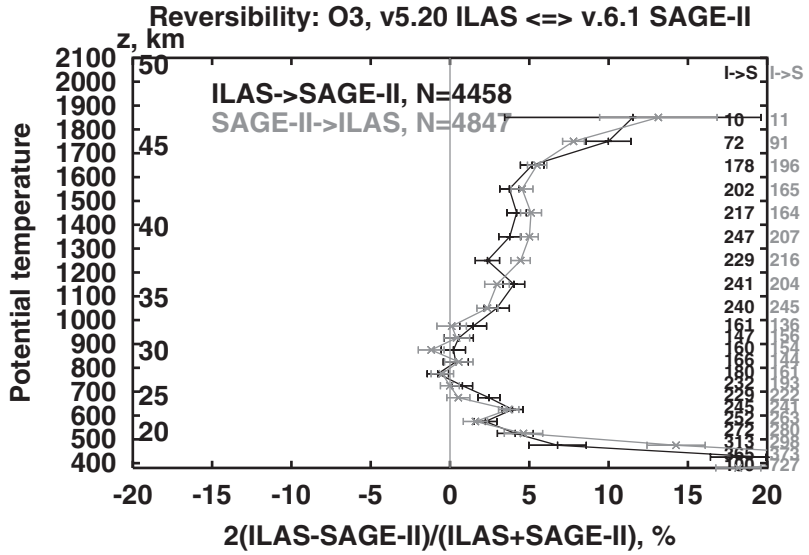

Figure 4. Black and gray lines show the difference between ILAS and SAGE-II ozone measurements for the trajectories launched from the ILAS and SAGE-II points, respectively. Similarity between these lines demonstrates the reversibility of THT. The vertical profiles of the number of matches are shown near the right vertical axis.

O_3 or HNO_3 along each matched trajectory. However, this approach has several drawbacks. First, it is difficult to get sufficient constraints for our model calculations. For example, MLS, POAM-II, and SAGE-II do not measure any tracer, thus disallowing us to get NO_y, Cl_y, and Br_y. Even knowing N_2O or CH_4 from the measurements, the NO_y-N_2O, NO_y-CH_4, Cl_y N_2O, and Cl_y CH_4 correlations scan easily introduce uncertainties of tens of percent [*Michelsen et al.*, 1998] in the stratosphere. Second, our model calculations can suffer from errors in initial partitioning of the nitrogen, chlorine, and bromine families, which are measured at best partially. Third, since THT provides tens of thousands of matches, the photochemical calculations require considerable computer resources. While we acknowledge the usefulness of the photochemical model calculations in the framework of the THT [*Danilin et al.*, 2002], we think that the analysis of additional uncertainties introduced by such calculations is beyond the scope of this paper.

[26] A more practical approach for assessing the effects of photochemistry on ozone comparisons is to analyze the results for ozone and any other passive traver (like H_2O) simultaneously for the same pair of instruments. The obvious advantage of this approach is that there is no need to run a photochemical box model, thus avoiding additional uncertainties introduced by the photochemical calculations. The ozone results contain both photochemical effects and THT noise. On the other hand, the water vapor results contain only the THT noise because of the long photo-

Table 2. Statistical Data for the Ozone Measurements Using THT[a]

Pair	Match Criterion	N_{tra}[b]	N	N_b	N_f	N/N_{tra}	$\overline{\Delta t}$, days	$\overline{sun}$, days
HALOE/ILAS[c]	2 h, 2°, 2°	15,782	2,523	1,557	966	0.2	1.7	1.5
HALOE/MLS	4 h, 2°, 2°	9,174	14,998	7,080	7,908	1.6	2.3	1.3
HALOE/POAM-II	2 h, 2°, 2°	4,002	129	129	0	0.0	3.7	2.7
HALOE/SAGE-II	6 h, 4°, 4°	7,871	9,064	1,791	7,273	1.2	1.9	1.6
ILAS/MLS	6 h, 2°, 2°	6,192	54,451	34,283	25,168	8.8	2.2	1.9
ILAS/POAM-II	2 h, 2°, 2°	8,244	4,823	3,892	931	0.6	3.5	2.7
ILAS/SAGE-II	2 h, 2°, 2°	22,478	4,458	1,914	2,544	0.2	1.8	1.4
POAM-II/MLS	6 h, 2°, 2°	4,700	36,730	19,510	17,220	7.8	2.3	1.9
SAGE-II/POAM-II	3 h, 2°, 2°	5,670	2,382	1,000	1,382	0.4	1.9	1.5
SAGE-II/MLS	2 h, 2°, 2°	25,600	53,720	26,893	26,827	2.1	2.2	1.8
SAGE-II/MLS[d]	2 h, 2°, 2°	25,600	14,551	5,808	8,743	0.6	0.4	0.3
SAGE-II/MLS	0.5 h, 0.5°, 0.5°	25,600	1,999	973	1,026	0.1	2.2	1.8
HALOE/HALOE	2 h, 2°, 2°	46,850	2,243	1,141	1,102	0.1	2.1	1.4
ILAS/ILAS	2 h, 2°, 2°	24,408	3,895	1,943	1,952	0.2	2.5	1.9
POAM-II/POAM-II	2 h, 2°, 2°	5,300	626	320	306	0.1	2.8	1.9
SAGE-II/SAGE-II	2 h, 2°, 2°	30,240	7,026	3,533	3,493	0.2	2.2	1.5

[a] Shown are the match criterion used (second column), the total number of relevant trajectories N_{tra} and matches N, number of matches for the backward (N_b) and forward (N_f) trajectories, number of matches per trajectory launched (N/N_{tra}), mean temporal distance between the matches ($\overline{\Delta t}$, days) and mean duration of sunlit conditions ($\overline{sun}$, days).

[b] Only trajectories within ±5days and ±10° of latitude from targets are counted.

[c] Trajectories are originated from and targeted to the location of the first and second instruments, respectively.

[d] One-day trajectories are used.

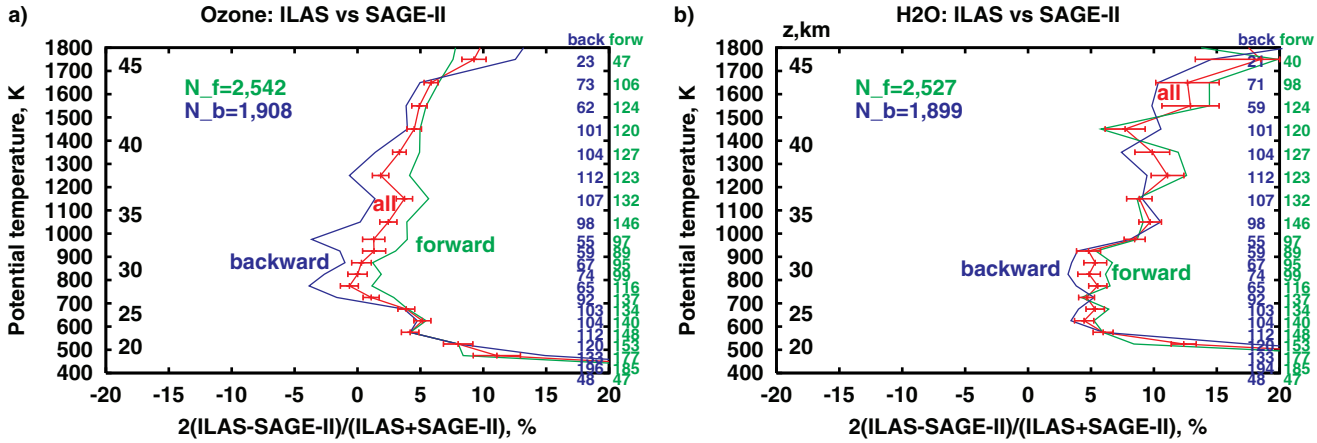

Figure 5. Contributions of the backward (blue line) and forward (green line) trajectories to the resulting difference (red line) between ILAS and SAGE-II measurements of ozone (top panel) and water vapor (bottom panel). Vertical distributions of the number of matches are shown near the right vertical axis. Total numbers of matches for the backward and forward trajectories are denoted as N_b and N_f, respectively.

chemical lifetime of H_2O and warm (i.e., above the ice frost point) temperatures along the matched air trajectories (which preclude rapid condensation of H_2O). Thus, the effects of photochemistry may be estimated based on the difference of the spread between forward and backward trajectories for the ozone results and a similar spread for the water vapor results.

[27] Figure 5 shows the results of the ozone (top panel) and water vapor (bottom panel) comparison of the ILAS and SAGE-II measurements. A spread of 4–8% between the ozone results for the forward and backward trajectories is obtained between 25 and 40 km. This spread is caused by the seasonal reduction of ozone at these altitudes near 70°S–80°S in November. Thus, the effects of photochemistry and THT noise for the "all" curve is about 2–4% (i.e., half of the spread). Bearing in mind a photochemical reduction of ozone with time, the forward trajectories launched from the ILAS locations tend to capture apparently reduced ozone values at the SAGE-II locations. For the backward ILAS trajectories, the situation is opposite (i.e., the ILAS O_3 measurements appear smaller at the locations of matches with SAGE-II). Since photochemical effects have opposite signs for the backward and forward trajectories, the ILAS-SAGE-II difference tends to be larger (smaller) for the forward (backward) trajectories. It is important to have the numbers of matches for the forward and backward trajectories about the same for the ozone comparisons, since a bias of one instrument versus another is defined as the sum of the differences for each match along backward and forward trajectories. If the numbers of matches for backward and forward trajectories are about the same, a possible photochemical increase or decrease of O_3 with time should be compensated. Otherwise, the total bias leans toward the results for the direction with larger numbers of matches.

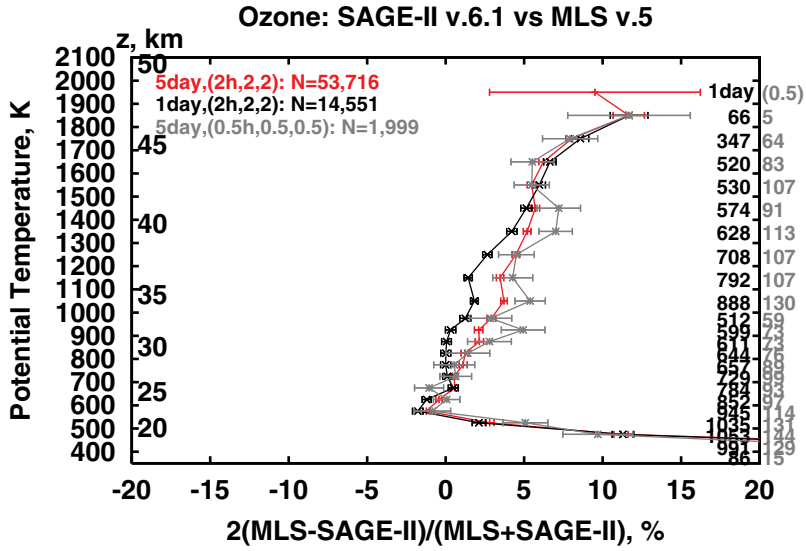

Figure 6. Sensitivity of the MLS/SAGE-II O_3 comparison to the match criterion chosen and the duration of the trajectories used: (red line) 5-day trajectories and (2 h, 2°, 2°), (black line) 1-day trajectories and (2 h, 2°, 2°), and (grey line) 5-day trajectories and (0.5 h, 0.5°, 0.5°).

Thus, analyzing only forward or backward trajectories for ozone comparisons, one can get an error of about 5% using 5-day trajectories. The necessity to use backward and forward trajectories together for ozone validation studies was also acknowledged by *Morris et al.* [2000].

[28] If there is not a systematic photochemical change in the ozone profile, then the results for the backward and forward trajectories should randomly intersect each other at different altitudes. For example, such a pattern is obtained for the water vapor results, additionally confirming that H_2O is a good inert tracer during this period. The magnitude of the spread between backward and forward trajectories for H_2O below 43 km is ~1–2%. Thus, photochemistry alone may affect the ozone results by up to 4%. Very similar results are seen for other instrument pairs of ozone measurements (not shown below).

4.4. Sensitivity to Match Criterion and Duration of Trajectories

[29] To investigate the sensitivity of the THT results to the duration of the trajectories used and the match criterion applied, we compare results of the ozone measurements made by MLS and SAGE-II. We pick this pair of instruments because of the very large number of matches (N = 53,716) obtained even for the relatively tight match criterion of (2 h, 2°, 2°). Figure 6 shows the difference between the MLS and SAGE-II O_3 measurements for the 5-day trajectories with the match criterion of (2 h, 2°, 2°) (red line) and (0.5 h, 0.5°, 0.5°) (grey line), and 1-day trajectories with the match criterion of (2 h, 2°, 2°) (black line). The similarity of these three curves is the most important feature of Figure 6, showing relatively weak sensitivity (less than 3%) to the duration of trajectories or match criteria used. In our previous study [*Danilin et al.*, 2002], we also obtained a weak sensitivity of the MLS/SAGE-II ozone results in February 2000 to the duration of the trajectories used. For the shorter trajectories or the tighter match criterion, the number of matches drops by a factor of 4 and 27, respectively, which leads to larger error bars in these cases. Figure 6 confirms that the possible errors in trajectory calculations do not affect noticeably (i.e., no more than 3%) our results.

4.5. Brief Summary of Section 4

[30] Quantifying the impact of uncertainties of the THT on the ozone results, we estimate that: (1) photochemical effects are the strongest among the sources of uncertainties and may contribute up to 4% for 5-day trajectories;(2) choice of the match criteria and duration of trajectories may affect the ozone results by up to 3%; (3) self-hunting tests show that uncertainties in trajectory calculations and various interpolations specific for THT usually affect ozone results by 1.7% in the stratosphere. Thus, the total THT uncertainty of the comparison of ozone measurements made by different instruments is about 3–5% at the 1-σ level. One should keep in mind that these values are valid for the atmospheric conditions of this study and may vary for different species and for different latitudes and seasons. For example, in the lower stratosphere at midlatitudes a photochemical lifetime of ozone is long (~months), thus eliminating the contribution of the photochemical term and providing a total uncertainty of 2–3% for the THT there.

[31] Summarizing the sensitivity studies performed in this section, we conclude that neither the uncertainties in the trajectory calculations, nor the possible photochemical changes along matched trajectories, nor the duration of the trajectories, nor the match criterion used affect our results noticeably and that the THT results are real and quite stable.

5. Comparison of the Ozone Measurements

[32] Ozone is a species measured by many satellites because of its importance as an ultraviolet shield protecting the Earth's biosphere and a radiatively active gas that is crucial for climate studies. Principal references dealing with O_3 measurements and validation are shown in Table 1. In comparing measurements made by MLS with four other instruments, one should keep in mind that the sampling volume of MLS (400 × 400 × 4 km^3) is typically larger by an order of magnitude than that of the occultation instruments (e.g., 200 × 60 × 1 km^3 for POAM-II). Thus, sampling volume differences may affect the comparison of the species of interest. However, such differences should be mitigated by the fact that a larger number of the matches is obtained using the THT and should not affect our conclusions.

[33] Figure 7 shows both the THT and TCA results for the ozone measurement comparisons depicted by the black and grey curves, respectively. Because of the sampling geometry of each instrument, the number of matches and match criteria differ for each pair. The loosest and tightest match criteria are (6 h, 4°, 4°) for the HALOE/SAGE-II pair and (2 h, 2°, 2°) for several other pairs, respectively. We are forced to relax our match criterion for some pairs in order to get at least several matched profiles using the TCA. There are two striking features of Figure 7: (1) good agreement between the TCA and THT results and (2) considerably smaller error bars on the THT curves. Indeed, the TCA comparison may look inconclusive in most cases, since the differences between the matched profiles are not statistically significant even at the 1 σ level because of the poor statistics obtained.

[34] It is impressive that the results provided by these techniques agree within their error bars almost everywhere in the stratosphere and for each pair. This fact may be considered as a validation of the THT using the TCA results and a justification of the THT credibility. On the other hand, TCA results also benefit from their agreement with THT, showing that TCA provides credible results despite its typically poor statistics. Previously, an agreement between the TCA and THT results was also obtained in a comparison of the MLS/SAGE-II and MLS/POAM-III ozone measurements during SOLVE [*Danilin et al.*, 2002]. However, the number of instruments involved and the number of matches

Figure 7. (opposite) Comparison of the ozone measurements by HALOE, ILAS, MLS, POAM-II, and SAGE-II using THT and TCA. Numbers of THT matches and approximate altitude in km are shown near the right and left vertical axes, respectively. The match criteria used are shown in each panel along with the number of matches for all (N), backward (N_b), and forward (N_f) trajectories for THT. The number of matched "profiles" in THT, $N_{\text{pro}}^{\text{THT}}$, is defined as N/N_{lev} (N_{lev} is the number of levels where the matches occurred), and the efficiency of THT is defined as $EFF = N_{\text{pro}}^{\text{THT}}/N_{\text{pro}}^{\text{TCA}}$. See text for details.

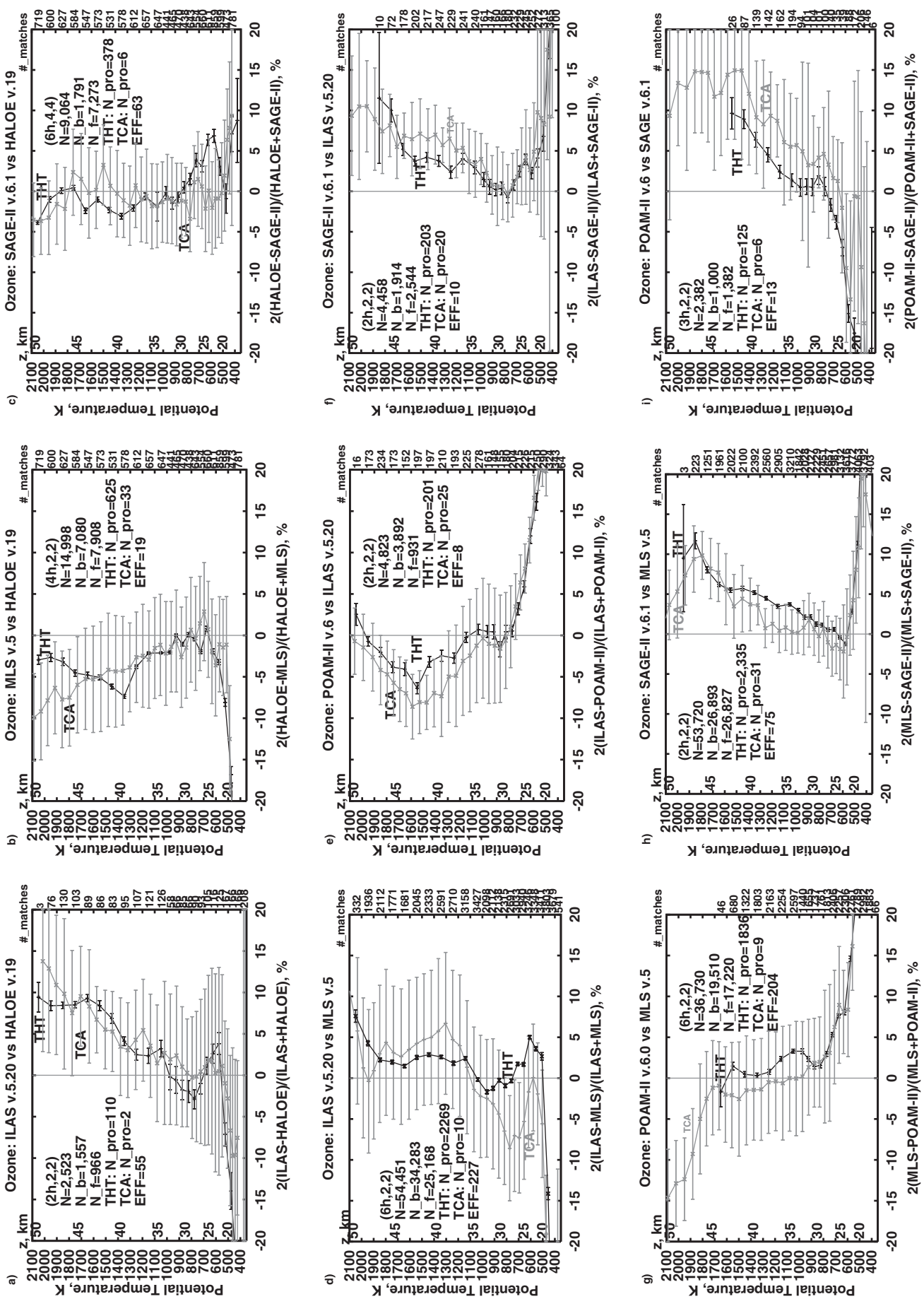
a)
Ozone: ILAS v.5.20 vs HALOE v.19
(2h,2,2)
N=2,523
N_b=1,557
N_f=966
THT: N_pro=110
TCA: N_pro=2
EFF=55
THT
TCA
2(ILAS-HALOE)/(ILAS+HALOE), %
b)
Ozone: MLS v.5 vs HALOE v.19
(4h,2,2)
N=14,998
N_b=7,080
N_f=7,908
THT: N_pro=625
TCA: N_pro=33
EFF=19
THT
TCA
2(HALOE-MLS)/(HALOE+MLS), %
c)
Ozone: SAGE-II v.6.1 vs HALOE v.19
(6h,4,4)
N=9,064
N_b=1,791
N_f=7,273
THT: N_pro=378
TCA: N_pro=6
EFF=63
THT
TCA
2(HALOE-SAGE-II)/(HALOE+SAGE-II), %
d)
Ozone: ILAS v.5.20 vs MLS v.5
(6h,2,2)
N=54,451
N_b=34,283
N_f=25,168
THT: N_pro=2269
TCA: N_pro=10
EFF=227
THT
TCA
2(ILAS-MLS)/(ILAS+MLS), %
e)
Ozone: POAM-II v.6 vs ILAS v.5.20
(2h,2,2)
N=4,823
N_b=3,892
N_f=931
THT: N_pro=201
TCA: N_pro=25
EFF=8
TCA
THT
2(ILAS-POAM-II)/(ILAS+POAM-II), %
f)
Ozone: SAGE-II v.6.1 vs ILAS v.5.20
(2h,2,2)
N=4,458
N_b=1,914
N_f=2,544
THT: N_pro=203
TCA: N_pro=20
EFF=10
THT
TCA
2(ILAS-SAGE-II)/(ILAS+SAGE-II), %
g)
Ozone: POAM-II v.6.0 vs MLS v.5
(6h,2,2)
N=36,730
N_b=19,510
N_f=17,220
THT: N_pro=1836
TCA: N_pro=9
EFF=204
TCA
THT
2(MLS-POAM-II)/(MLS+POAM-II), %
h)
Ozone: SAGE-II v.6.1 vs MLS v.5
(2h,2,2)
N=53,720
N_b=26,893
N_f=26,827
THT: N_pro=2,335
TCA: N_pro=31
EFF=75
TCA
THT
2(MLS-SAGE-II)/(MLS+SAGE-II), %
i)
Ozone: POAM-II v.6 vs SAGE v.6.1
(3h,2,2)
N=2,382
N_b=1,000
N_f=1,382
THT: N_pro=125
TCA: N_pro=6
EFF=13
THT
TCA
2(POAM-II-SAGE-II)/(POAM-II+SAGE-II), %
Potential Temperature, K
z, km
matches

found is much larger in this study, making the validation of the THT results robust. Surprisingly, the agreement between the THT and TCA ozone results holds even above 40 km, where the ozone photochemical lifetime is on the order of days or even hours near 50 km. Perhaps the agreement for the POAM-II/ILAS pair may be understood by assuming that ozone is in steady state, meaning that O_3 values should be the same at sunset, when these measurements are taken. For all other pairs, we see perhaps a fortunate disappearance of effects of the ozone diurnal variability in the upper stratosphere in our results.

[35] Very large statistics is a big advantage of the THT. Figure 7 illustrates that the TCA results quite often are not statistically significant (i.e., the grey error bars cover the zero vertical line) in the stratosphere (particularly for the SAGE-II/HALOE and ILAS/MLS comparisons). This is a consequence of the small number of matched profiles. On the other hand, THT finds approximately 100 times more matches during this period, thus making the THT results statistically more robust due to ~10 times smaller error bars (since the error bars are reduced by a factor of $N^{-1/2}$ according to (1)). This fact makes the THT particularly attractive for analysis of sparse data (like balloon or aircraft flights and occultation satellite measurements) or for short data sets. However, the error bars shown for the THT results in our study are defined according to equation (1) (i.e., in same way as the TCA error bars) and do not account for the uncertainties of trajectories calculations or ignorance of the photochemical changes. To account for these uncertainties, the THT error bars should be increased by 1–2%.

[36] In order to quantify the statistical efficiency of the THT compared to the TCA, we introduce the parameter EFF defined as the ratio of the profiles matched by THT, $N_{\mathrm{pro}}^{\mathrm{THT}}$, to that by TCA, $N_{\mathrm{pro}}^{\mathrm{TCA}}$, according to:

$$EFF = \frac{N_{\mathrm{pro}}^{\mathrm{THT}}}{N_{\mathrm{pro}}^{\mathrm{TCA}}}. \quad (3)$$

The caveat of this definition is that $N_{\mathrm{pro}}^{\mathrm{THT}}$ is defined as the total matches obtained N using the THT divided by the number of levels N_{lev} where the THT matches were grouped. In contrast to the TCA, the THT "profile" is just a useful term for quantifying the efficiency of THT against TCA and should not be considered literally, since different THT matches are obtained at different levels and quite likely they do not belong to the same original profiles. The values of the EFF parameter range from 8 for the ILAS/POAM-II pair to 204 for the MLS/POAM-II pair. Relatively small values of EFF typically indicate that the instruments made measurements close to each other and the TCA is able to find a relatively large number of matched profiles for this pair of instruments. Large EFF values signal that these pairs of instruments had different sampling geometries. In terms of the number of matches, comparisons with MLS are dominant because of the almost 50 times more frequent sampling pattern of MLS (i.e., ~1300 profiles/day versus 28 profiles/day for all four occultation instruments).

[37] Table 2 provides detailed statistics quantifying the THT comparison of the ozone measurements made by different instruments. Table 2 confirms that one gets more matches for trajectory hunting against more frequent measurements and with more relaxed match criteria. Indeed, the number of matches per trajectory launched (N/N_{tra}, the third column from the right) is larger for the hunting against the MLS measurements, ranging from 1.6 (HALOE/MLS pair) to 8.8 (ILAS/MLS pair). This ratio is the largest for the ILAS/MLS and POAM-II/MLS pairs because the hunting is performed near 75°S, where the targeted measurements are more dense compared with the tropics (HALOE/MLS pair) or midlatitudes (SAGE-II/MLS pair). The N/N_{tra} ratio drops considerably for the hunting against the occultation instruments. This ratio is also reduced for a tighter match criterion or shorter trajectories (see the SAGE-II/MLS lines). The mean time between THT matches ranges from 1.7 to 3.7 days and is about 2.5 days on average for all pairs, or about half of the 5-day trajectories. Very similar results were obtained in our analysis of the SOLVE data [*Danilin et al.*, 2002]. One may speculate that matches are obtained more or less homogeneously along trajectories and the mean value of the time between matches is about half of the trajectory duration used for the analysis. The sunlit conditions along the matched trajectories are quantified by the last column. The sunlit values are sensitive to season and latitude and are maximum for the POAM-II/MLS pair (i.e., near 75°S) and minimum for the HALOE/MLS pair (i.e., in the tropics).

Table 3. PV Values of the Polar Vortex Edge and Numbers of HALOE, ILAS, MLS, POAM-II, and SAGE-II Ozone Measurements[a]

θ, K	PV	HALOE	ILAS	MLS	POAM-II	SAGE-II
425	0.17	239	663	3,586	967	3,475
475	0.28	219	587	3,692	1,378	3,120
525	0.42	219	510	3,393	1,234	2,876
575	0.62	163	439	3,349	1,129	2,882
625	0.89	135	413	2,879	988	2,449
675	1.30	121	377	2,771	908	2,373
725	1.88	102	345	2,262	883	1,848
775	2.56	109	279	1,926	628	1,664
825	3.27	61	264	1,840	629	1,568
875	4.26	64	209	1,643	509	1,425
925	5.34	52	179	1,615	494	1,414
975	6.58	42	169	1,396	389	1,256
1,050	9.15	62	228	1,935	481	1,798
1,150	13.5	26	85	1,074	185	1,020
1,250	18.9	0	27	383	63	353
1,350	24.1	0	27	402	50	381
1,450	29.0	0	29	344	48	323
Total	–	1,614	4,830	34,490	10,963	30,225

[a] PV values are in 10^{-4} PV units, temperature in Kelvin. The total numbers of the HALOE, ILAS, MLS, POAM-II, and SAGE-II ozone measurements inside the vortex used in Figure 8 as a function of potential temperature θ are given.

[38] In order to compare simultaneously the multiplatform ozone measurements, we follow the methodology outlined by *Manney et al.* [2001]. They used potential vorticity (PV) as a helpful flag to segregate different air masses and applied the fact that long-lived gases are well-correlated with PV [e.g., *Manney et al.*, 1999]. The core of the polar night jet is characterized by a region of strong PV gradients, which can be used to roughly indicate the edge of the vortex. The values of PV_v shown in the second column of Table 3 represent typical threshold values defining the edge of the polar vortex at each level during the 1990s period in the Southern Hemisphere. We will show below that our results comparing the ozone and water vapor measurements in the vortex are not sensitive to PV_v. The UK Meteorological Office (UKMO) PV values were assigned to all our matched

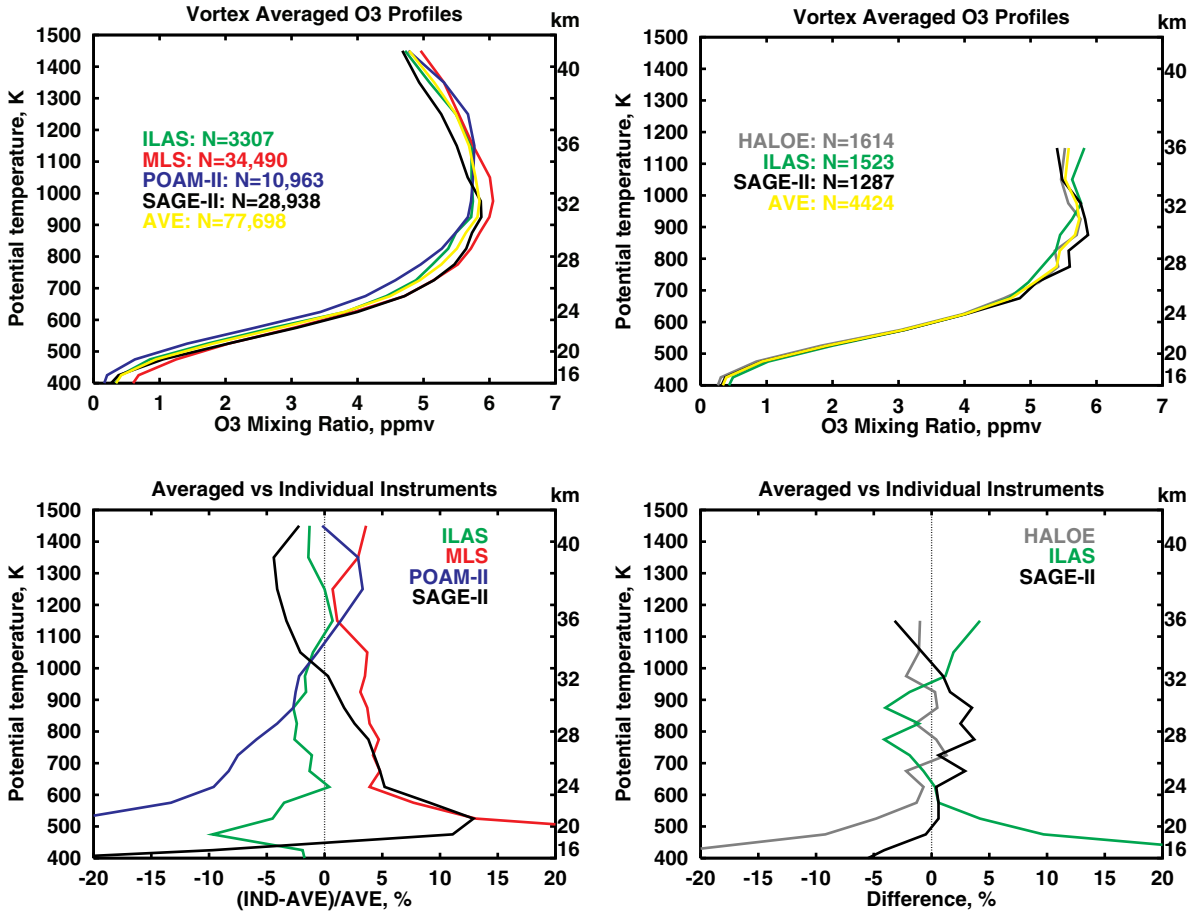

Figure 8. Comparison of the ozone measurements inside the vortex by HALOE, ILAS, MLS, POAM-II, and SAGE-II using the THT at the beginning of November (left column) and second half of November (right column): (top panel) mean O_3 profile by each instrument and their averaged profile (black line); difference of each instrument from the averaged profile in % (bottom panel).

measurements. We selected a subset of the matched ozone measurements made by all instruments that have PV values larger than PV_v. In contrast to the *Manney et al.* [2001] study, we did not relax the match criterion in order to get more matches. Moreover, we used the same match criterion of (2 h, 2°, 2°) for all pairs, thus reducing the number of matches for HALOE/SAGE-II, ILAS/MLS, POAM-II/MLS, and POAM-II/SAGE-II pairs (since more relaxed match criteria were used for these pairs in Figure 7). Once the matched ozone measurements in the vortex are identified, we assume a homogeneous ozone field within the vortex and thus no additional separation among these measurements as a function of PV or latitude is needed. The total numbers of the HALOE, ILAS, MLS, POAM-II, and SAGE-II measurements as a function of potential temperature involved in the comparison inside the polar vortex are listed in Table 3.

[39] Figure 1 shows that there are two distinctly different matching events centered near 5 November (the ILAS, MLS, POAM-II, and SAGE-II O_3 measurements are involved) and 22 November (the ILAS, SAGE-II, and HALOE O_3 measurements are involved). Since the ozone field evolved from 5 November to 22 November, we decided to split our analysis into these two periods in order to ensure that ozone was constant during each of them.

[40] The mean ozone profile in the vortex, AVE_j, at the jth vertical level was determined according to:

$$AVE_j = \frac{\sum_{i=1}^{all} I_{ij} \times N_{ij}}{\sum_{i=1}^{all} N_{ij}} \quad (4)$$

here I_{ij} is the mean ozone value of the ith instrument at the jth vertical layer, N_{ij} is the number of the ith instrument measurements at the jth vertical level, *all* is the total number of the instruments involved (*all* = 4 and *all* = 3 for the matching events near 5 November and 22 November, respectively).

[41] Figure 8 shows the comparison of the vortex ozone measurements for these two time periods. Such a simultaneous comparison of multiplatform measurements shows that using the THT we found a "common denominator", which allows us to understand better possible biases in the measurements instead of analyzing a set of individual pair differences. The top row of Figure 8 shows the vortex averaged ozone profiles made by each instrument. The vertical range of this figure is smaller than in Figure 7 because of the lack of measurements made simultaneously by all platforms in the vortex above 1500 K during the 5 November interval (left column) and above 1200 K during

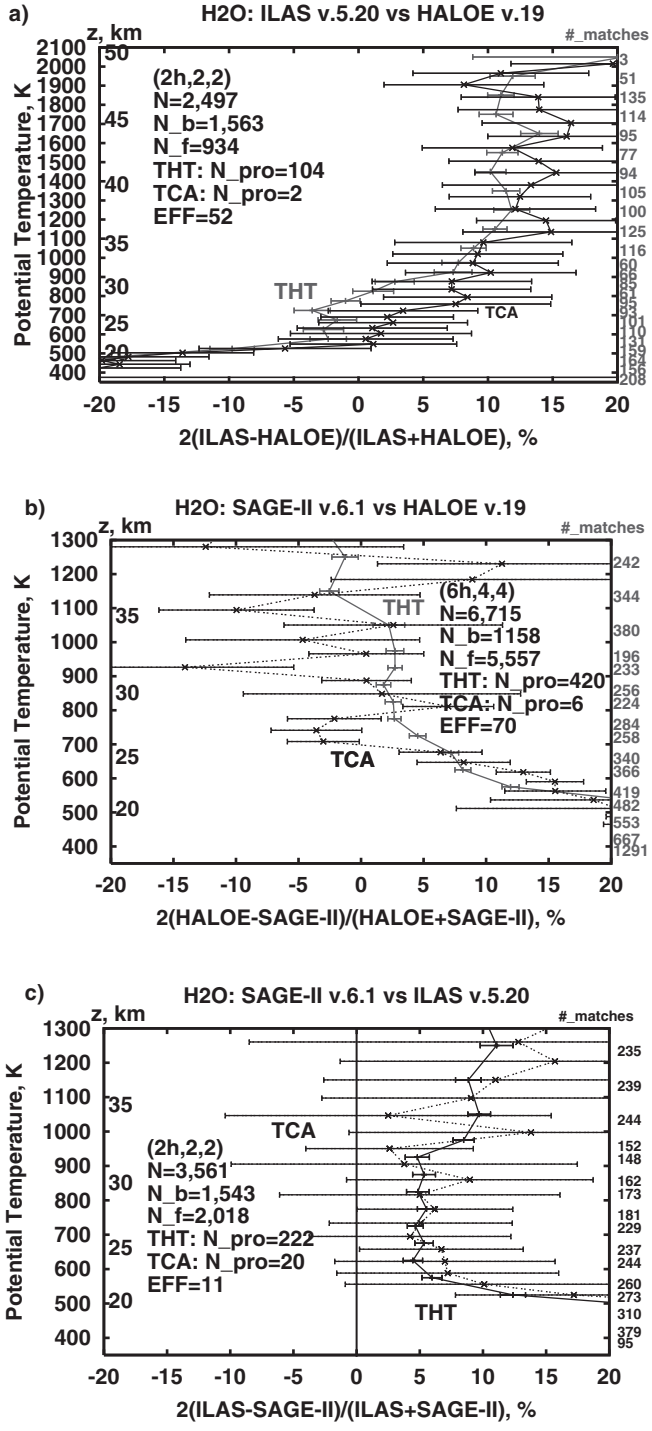

Figure 9. The same as in Figure 7, but for the ILAS, HALOE, and SAGE-II measurements of H_2O.

the 22 November interval (right column). The number of matches during the first interval is 18 times more than during the second because of the very frequent matched MLS measurements obtained at the beginning of November. The deviations of the individual instruments from the mean ozone profile are shown in the bottom (in %) row of Figure 8. In general, the agreement between the ozone measurements is within ±5% (or ±0.2 ppmv) above 28 km during the first event. In the lower stratosphere the differences are larger, reaching −0.4 and +0.3 ppmv for the POAM-II and MLS measurements, respectively. Agreement between the ILAS, HALOE, and SAGE-II ozone measurements is even better (within ±5% or 0.2 ppmv above 20 km) during the second matching event.

[42] We performed a sensitivity study of our results to the PV_v values. We obtained very similar results for PV_v values reduced or increased by 20% (not shown here). Thus, we concluded that our results in Figure 8 are not sensitive to the choice of the PV_v values. We did not compare the matched ozone values outside the polar vortex, since different air masses may be compared in this case. For example, MLS/SAGE-II matches could correspond to midlatitude or even tropical air masses, while subpolar air masses could be obtained for the ILAS/POAM-II pair.

[43] In general, results of our comparison of the ozone measurements are in reasonable agreement with more detailed validation studies performed by each of the instrument teams. For instance, the differences obtained here between MLS and SAGE-II ozone measurements are consistent with the conclusions by N. J. Livesey et al. (The UARS MLS version 5 dataset: Theory, characterization, and validation, submitted to *Journal of Geophysical Research*, 2002, hereinafter referred to as Livesey et al., submitted manuscript, 2002). Their study showed a small positive offset in the v.5 MLS measurements (0.1–0.2 ppmv) with larger relative effects at the lowest altitudes in the tropics. Negative offsets in the POAM-II O_3 measurements in the stratosphere were also previously documented. For example, *Rusch et al.* [1997] reported that POAM-II v.5 ozone data are systematically lower by up to 20% than the MLS v.3, HALOE v.17, and SAGE v.5.93 below 20 km. *Deniel et al.* [1997] also discovered a negative bias in the POAM-II v.5 O_3 measurements compared with ozonesonde profiles (albeit in the Northern Hemisphere) ranging from 2–3% near 17 and 30 km to 7.6% at 21–24 km. Our study shows a stronger negative bias in the POAM-II ozone measurements than those reported by *Rusch et al.* [1997] and *Deniel et al.* [1997]. However, direct comparisons of our and previous POAM-II validation studies should be done with care, since different versions of POAM-II, MLS, and SAGE-II measurements are used here than by *Rusch et al.* [1997] and *Deniel et al.* [1997]. Also, when a larger time period is used (i.e., 1994–1996 versus October–November 1996), the POAM-II v.6 negative offset against SAGE-II v.6.1 ozone data is smaller than that reported in this study (C. Randall, personal communication, 2002). The ILAS v.5.20 ozone measurements typically agree within ±10% with the balloon, aircraft, ground-based, HALOE, POAM-II, and SAGE-II measurements according to *Sugita et al.* [2002]. They also reported a possible positive bias of up to 10–15% in the ILAS measurements compared with the HALOE and SAGE-II measurements near 45–55 km, as detected in our study.

[44] Summarizing the major findings of this section, we want to highlight: (1) successful validation of the THT results based on their comparison with TCA data; (2) large statistics and consequently small error bars of the THT results allowing detection of small biases in different instrument measurements of O_3; and (3) good agreement of our

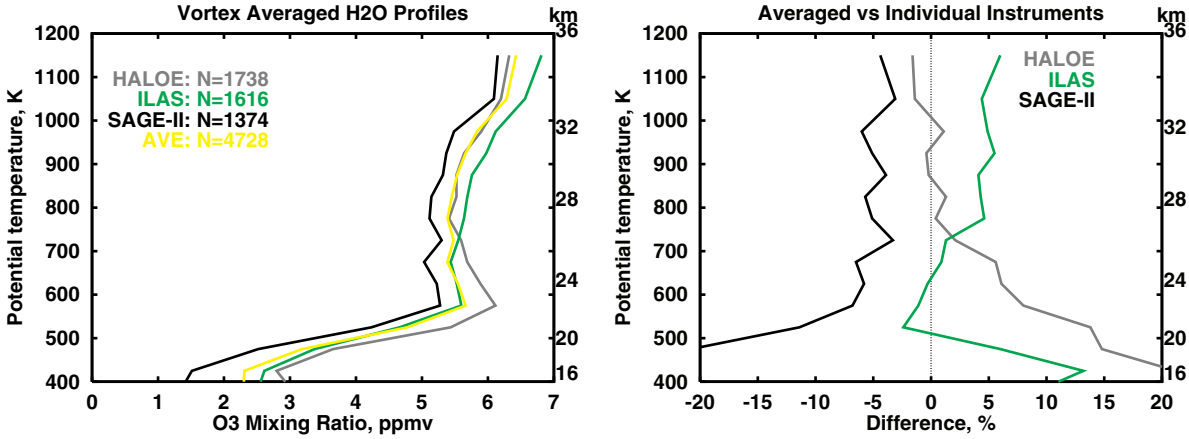

Figure 10. The same as in Figure 8, but for the ILAS, HALOE, and SAGE-II measurements of H_2O.

results using only this 40-day period with other special validation studies of the ozone measurements (using multi-year data sets). The small differences of order of a few tenths of ppmv, or several percent, obtained in our study show that the current satellite ozone measurements are quite accurate.

6. Comparison of the Water Vapor Measurements

[45] Among the five instruments considered in this study, only three (HALOE, SAGE-II, and ILAS) provided water vapor measurements during the 22 October to 30 November 1996 period. MLS H_2O measurements were available before the 183-GHz radiometer failure in April 1993 [*Lahoz et al.*, 1996; Livesey et al., submitted manuscript, 2002]. The POAM-II water vapor filter at 926 nm failed and no H_2O measurements were made. Water vapor measurements and their validation studies are listed in Table 1. Additionally, *Stratospheric Processes and Their Role in Climate* (*SPARC*) [2000] provided a very detailed study of all available water vapor measurements, including those made by HALOE, SAGE-II, and ILAS.

[46] Figure 9 shows the comparisons of water vapor measurements (in %) when both the THT (red lines) and TCA (black lines) are applied. Again, as in the ozone case, good agreement between these two techniques is obtained and the THT data are more statistically robust than those from the TCA. For instance, the TCA results are not statistically significant for the SAGE-II/ILAS pair event at the 1σ confidence level. In general, the THT results are smoother and closer to the zero vertical line because of its better statistics. Since water is photochemically inert in the stratosphere and no condensation or evaporation occurred, we compared the matched H_2O results directly.

[47] The vortex H_2O measurements by ILAS, HALOE, and SAGE-II, defined in the same way as the ozone vortex measurements in the previous section, are compared in Figure 10. Almost 6,000 individual H_2O measurements are involved and their mean profile is defined according to equation (4). The relative differences of the individual

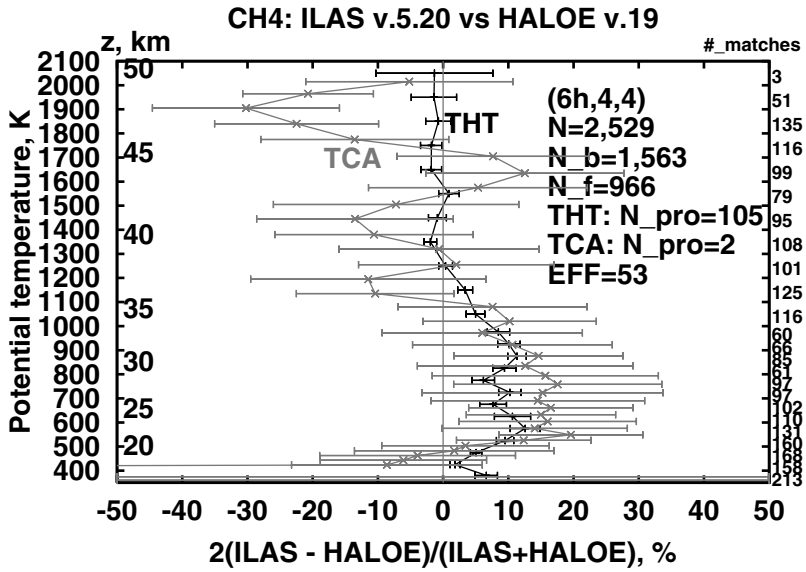

Figure 11. Profile of the difference between HALOE and ILAS measurements of CH_4 according to the TCA and THT.

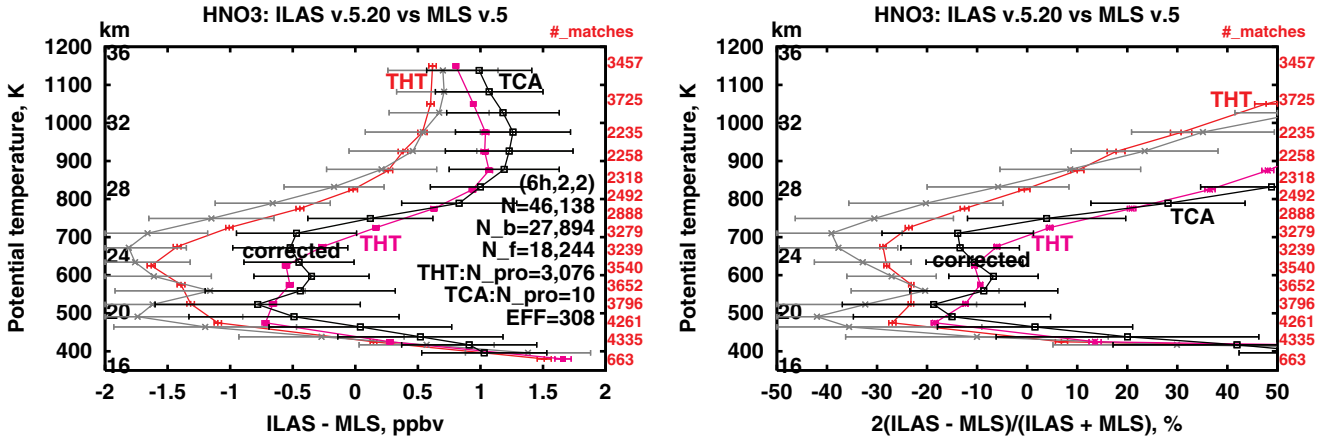

Figure 12. Profile of the difference between v.5 MLS and ILAS measurements of HNO_3 using TCA (grey lines) and THT (red lines). Results for the corrected v.5 MLS HNO_3 measurements are shown by the magenta and black lines for THT and TCA, respectively (see text for details). Other labels are the same as in Figure 7.

instruments from the mean profile are shown in the bottom panel of Figure 10. The agreement between all these instruments is remarkably good (better than 5%, or 0.2 ppmv) above 600 K (~23 km). Below 23 km, the differences become larger with a positive (negative) bias in HALOE (SAGE-II) measurements, which may be anticipated based on the Figure 9 results.

7. Comparison of the Methane Measurements

[48] Methane is measured by HALOE [*Park et al.*, 1996] and ILAS [*Toon et al.*, 2002; *Kanzawa et al.*, 2002]. CH_4 photolysis is caused mostly by the solar radiation at Lyman-α (121.6 nm), which barely penetrates into the stratosphere. Thus, methane has a photochemical lifetime longer than several years in the stratosphere (since the CH_4 + OH reaction is also very slow) and can be treated as a good passive tracer in the context of our study.

[49] Figure 11 depicts the vertical profile of the relative difference (in %) between the ILAS and HALOE measurements of CH_4. Both techniques confirm that the ILAS values are higher than those by HALOE below 35 km, reaching a maximum difference of almost 20% (11%) near 22 km using the TCA (THT). The THT results show better agreement between the ILAS and HALOE CH_4 measurements, which may be attributed to better statistics in the THT case. Above 35 km, the THT could not detect a statistically significant difference between these measurements. Our THT results agree with the statement that HALOE and available correlative CH_4 measurements agree within 15% [*Park et al.*, 1996]. Also, our findings agree well with the conclusions by *Kanzawa et al.* [2002], which showed higher ILAS values by 10–15% below 35 km in the Southern Hemisphere.

8. Comparison of the Nitric Acid Measurements

[50] Nitric acid is measured by MLS [*Santee et al.*, 1999, 2000; Livesey et al., submitted manuscript, 2002] and ILAS [*Koike et al.*, 2000; *Irie et al.*, 2002]. After the MLS v.5 data set was produced it was discovered that emissions from the HNO_3 ν_9 and ν_7 excited vibrational states, which were omitted from the v.5 retrieval system, are significant in the spectral region in which MLS HNO_3 is being retrieved. Neglecting the contributions from these lines caused the retrieved MLS values to significantly overestimate stratospheric HNO_3 abundances. An empirical correction to the MLS v.5 HNO_3 data set has been derived and is described in detail by Livesey et al. (submitted manuscript, 2002). We compare both the original v.5 and the corrected v.5 MLS HNO_3 values with those from ILAS. This correction does not affect our comparisons for the MLS v.5 O_3 measurements.

[51] Figure 12 shows the ILAS/MLS HNO_3 comparisons in ppbv (top panel) and in % (bottom panel) using TCA and THT. Comparisons using both the original and the corrected v.5 MLS HNO_3 mixing ratios are shown. Both the TCA and the THT techniques produce similar results, although the THT results are more statistically significant. Large differences (exceeding 1.5 ppbv at some levels) are apparent between ILAS and MLS v.5 values over the range ~450–750 K. Similar differences have been noted previously between MLS data and those from other spaced-based [*Santee et al.*, 2000; *Danilin et al.*, 2000] and airborne instruments [*Danilin et al.*, 2002]. Applying the empirical correction to account for the neglect of the excited vibrational states in the MLS v.5 retrievals reduces the discrepancy with ILAS to ~0.5 ppbv (~10–20%) over the 450–750 K range. Above ~750 K, however, the corrected MLS data exhibit worse agreement with ILAS, with offsets between the two data sets of about 1 ppbv. A similar low bias in MLS HNO_3 data at 740 K and 960 K has been seen in comparisons with HNO_3 measurements from a ground-based microwave instrument at the South Pole [*Muscari et al.*, 2002] and from CLAES. The small HNO_3 mixing ratios at these altitudes and in the lowermost stratosphere, where the difference with ILAS is also about 1 ppbv, lead to large percent differences in these regions. On the other hand, *Irie et al.* [2002] found good agreement (to better than ±0.5 ppbv) between ILAS v.5.20 HNO_3 and balloon measurements at 15–35 km.

[52] Nitric acid has a photochemical lifetime of at least several days below 35 km [*Brasseur and Solomon*, 1984],

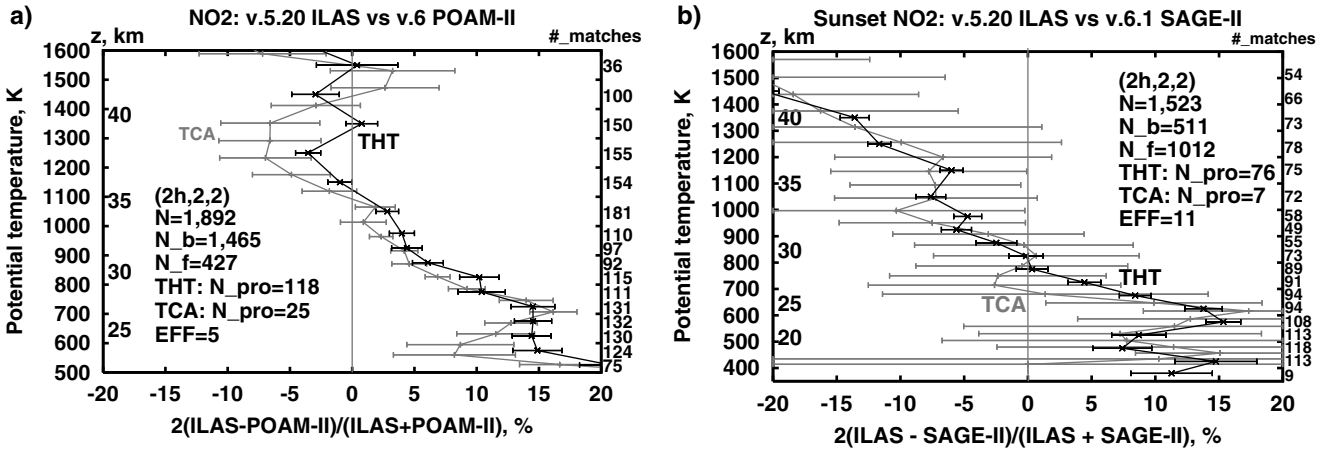

Figure 13. Comparison of the ILAS/POAM-II (top panel) and ILAS/SAGE-II NO_2 (bottom panel) sunset measurements. A steady state is assumed for the ILAS/POAM-II and ILAS/SAGE-II comparisons. Sunrise SAGE-II and sunset POAM-II NO_2 measurements in the beginning of November could not be compared directly and are not shown.

i.e., comparable to the mean temporal distance of 2.3 days obtained for the THT results. In order to estimate photochemical effects on the HNO_3 results, we analyze the THT results separately for the backward and forward trajectories originating from the ILAS locations (not shown in Figure 12). The spread between the backward and forward trajectory results is small ($\sim$0.1–0.2 ppbv) and consistent with the analysis by *Santee et al.* [1999] showing that the HNO_3 values in the lower stratosphere near 70°S in November are almost constant. Thus, photochemistry has small effects on the ILAS/MLS HNO_3 measurement comparison during the period considered.

9. Comparison of the Nitrogen Dioxide Measurements

[53] Nitrogen dioxide is measured by HALOE [*Gordley et al.*, 1996], ILAS [*Irie et al.*, 2002], POAM-II [*Randall et al.*, 1998], and SAGE-II [*Cunnold et al.*, 1991]. Nitrogen dioxide is not a long-lived species and has strong diurnal variability in the stratosphere. This means that without a photochemical box model only measurements made at the same local time (either sunrise or sunset) may be compared. Figure 1 shows that only sunset NO_2 measurements made by POAM-II, ILAS, and SAGE-II can be compared during the period considered. To justify direct comparison of the sunset ILAS, SAGE-II, and POAM-II NO_2 measurements, we assume that NO_2 is in steady state. We think that this assumption is valid since: (1) NO_y is constant (no denitrification occurs along the matched trajectories); (2) HNO_3 and ozone did not change considerably during a typical interval of 2–3 days between the matches (see the above sections dealing with O_3 and HNO_3 measurement comparisons); and (3) the temperature was about the same in the initial and final points of the matches (indeed, we found about 2–4 K difference). Previous calculations [*Kawa et al.*, 1993; *Salawitch et al.*, 1994] show that these three conditions provide a steady state in the stratosphere.

[54] Figure 13 shows the comparison of the ILAS/POAM-II (top panel) and ILAS/SAGE-II (bottom panel) sunset NO_2 measurements. The sunset POAM-II and SAGE-II NO_2 measurements can not be compared because of the large temporal difference between them (see Figure 1). Again, as in all previous sections, we obtained good agreement between the TCA and THT results and good statistics for the THT, leading to their small error bars. Figure 13a shows the very good agreement (i.e., better that ±5%) between ILAS and POAM-II sunset NO_2 measurements was obtained above 30 km. However, the strongest disagreement of $\sim$15% (or 0.4–0.5 ppbv) was obtained in the lower stratosphere. The results shown in Figure 13a are very similar to those by *Irie et al.* [2002]. Their more detailed comparisons with the balloon measurements show that ILAS has a positive bias below 35 km, which was attributed to the lack of diurnal correction of NO_2 in the ILAS retrieval. However, the reasons for the POAM-II/ILAS discrepances in the lower stratosphere are not clear, since POAM-II also does not account for diurnal correction of NO_2.

[55] ILAS sunset NO_2 measurements are larger than SAGE-II v.6.1 values up to 10–15% below 30 km (see Figure 13b). Since a similar difference was observed for ILAS/POAM-II, one may speculate that the POAM-II and SAGE-II sunset NO_2 measurements are in good agreement below 800 K ($\sim$27 km). Above 35 km, the SAGE-II NO_2 measurements tend to be larger by more than 10% (or up to 1 ppbv), suggesting a possible positive bias in the v.6.1 SAGE-II NO_2 data. This possible high bias in the SAGE-II measurements in the upper stratosphere is also suggested by the small difference (less than 10%) between the ILAS and POAM-II NO_2 measurements. More detailed validation of the latest version of the SAGE-II NO_2 measurements is underway. Our study shows that the SAGE-II NO_2 retrieval is considerably improved in v.6.1 compared with that in v.6.0, which showed NO_2 values that were too high by several ppbv in the stratosphere.

10. Summary and Outlook

[56] Our study presents a detailed description of the trajectory hunting technique. Several consistency tests were

performed for the THT (e.g., self-hunting). We found that the possible biases associated with the THT are of order of 1–2% for O_3, CH_4, and H_2O, and 4% for NO_2 and HNO_3 data based on the self-hunting results. THT has the property of reversibility, showing that the choice of hunter and target is not important. The THT results are stable (within ~2% for O_3 comparisons) with regard to the match criteria and duration of the trajectories used. Analyzing simultaneously the ILAS and SAGE-II O_3 and H_2O measurements, we estimate that photochemical processes could affect the ozone results in the mid to upper stratosphere by up to 4%. However, this value is valid only for the conditions of this study and depend on latitude, season, and altitude.

[57] We validated the THT by comparing its results against the TCA results for ozone, water vapor, methane, nitric acid, and nitrogen dioxide measurements using the latest versions of MLS (v.5), HALOE (v.19), ILAS (v.5.20), SAGE-II (v.6.1), and POAM-II (v.6) during the 22 October to 30 November 1996 period. While the results for all these comparisons agree within their error bars, the THT results are more statistically robust because of the much larger number of matches obtained in this technique. Comparing these products using the THT we find:

1. Ozone measurements from all five platforms typically agree to better than 0.4 ppmv below 30 km and better than 0.2 ppmv above 30 km. MLS and POAM-II instruments showed a positive (negative) offset of +0.2 ppmv (up to −0.4 ppmv) from the mean in the lower stratosphere, respectively;

2. ILAS, HALOE, and SAGE-II water vapor measurements usually agree to better than 10% above 22 km with a small negative (positive) offset of SAGE-II (HALOE) in the lower stratosphere;

3. HALOE and ILAS methane measurements agree better than 10% above 30 km, with a positive offset of up to 10–15% in the ILAS measurements in the lower stratosphere;

4. MLS v.5 HNO_3 measurements show a large positive offset (up to 1.5 ppbv, or ~25–30%) relative to those from ILAS over the range ~450–750 K. Application of a correction accounting for some excited vibrational lines omitted in the MLS v.5 HNO_3 retrieval (Livesey et al., submitted manuscript, 2002) leads to revised MLS HNO_3 mixing ratios that agree to within about 0.5 ppbv (~10–20%) in this region. Above 750 K differences of about 1 ppbv are seen that may indicate a possible low bias in the corrected MLS HNO_3 retrievals.

5. Below 30 km, ILAS NO_2 sunset measurements are larger by 10–15% than both POAM-II and SAGE-II values, while SAGE-II NO_2 data show a positive offset above 35 km.

[58] Our findings regarding individual products agree well with the very detailed independent validation studies of the ozone [Livesey et al., submitted manuscript, 2002; *Sugita et al.*, 2002], water vapor [*Kanzawa et al.*, 2002], nitric acid [*Irie et al.*, 2002], and nitrogen dioxide [*Randall et al.*, 1998; *Irie et al.*, 2002] measurements. These studies typically cover several years of measurements in order to reveal statistically significant offsets between instruments. The THT requires only about a month of overlapping measurements in order to find statistically significant offsets (with some caveats associated with latitudinal and seasonal coverage) outside the 3–5% uncertainties introduced by the THT itself. The good agreement between the THT and TCA results for all species and instruments considered in this study confirms the credibility of the THT. Thus, the THT is indeed an effective technique for validation studies and may serve as a "statistical reinforcer" for the TCA. We believe that the THT is a very attractive technique for a quick and statistically robust validation of measurements made by a new instrument, especially if this instrument has a low frequency of measurements (like satellite occultation instruments or balloons).

[59] **Acknowledgments.** Work at AER, Inc. was supported by the UARS Guest Investigator Program (NAS5-98131 and NAS5-01162) and NASA ACMAP (NAS1-00138). Work at the Jet Propulsion Laboratory was done under contract with NASA. NCAR is supported by the National Science Foundation. The ILAS project is sponsored by the Ministry of Environment, Japan. We thank H. Kanzawa and T. Sugita for sending us their unpublished ILAS validation papers. We appreciate valuable comments of Cora Randall and three anonymous reviewers.

References

Austin, J., Comparison of stratospheric air parcel trajectories calculated from SSU and LIMS satellite data, *J. Geophys. Res.*, *91*, 7837–7851, 1986.

Austin, J., R. C. Pallister, J. A. Pyle, A. F. Tuck, and A. M. Zawody, Photochemical model comparisons with LIMS observations in a stratospheric trajectory coordinate system, *Q. J. R. Meteorol. Soc.*, *113*, 361–392, 1987.

Bacmeister, J. T., V. Kuell, D. Offermann, M. Riese, and J. W. Elkins, Intercomparison of satellite and aircraft observations of long-lived tracers using trajectory mapping, *J. Geophys. Res.*, *104*, 16,379–16,390, 1999.

Barath, F., et al., The UARS Microwave Limb Sounder Instrument, *J. Geophys. Res.*, *98*, 10,751–10,762, 1993.

Becker, G., R. Müller, D. S. McKenna, M. Rex, and K. S. Carslaw, Ozone loss rates in the Arctic stratosphere in the winter 1991/92: Model calculations compared with Matched results, *Geophys. Res. Lett.*, *24*, 4325–4328, 1998.

Bevilacqua, R. M., Introduction to the special section: Polar Ozone and Aerosol Measurement (POAM-II), *J. Geophys. Res.*, *102*, 23,591–23,592, 1997.

Brasseur, G. P., and S. Solomon, *Aeronomy of the Middle Atmosphere*, D. Reidel, Norwell, Mass., 1984.

Brühl, C., et al., HALOE ozone channel validation, *J. Geophys. Res.*, *101*, 10,217–10,240, 1996.

Chu, W. P., et al., Algorithms and sensitivity analyses for SAGE-II water vapor retrieval, *J. Geophys. Res.*, *98*, 4857–4866, 1993.

Cunnold, D. M., et al., Validation of SAGE-II NO_2 measurements, *J. Geophys. Res.*, *96*, 12,913–12,925, 1991.

Danilin, M. Y., et al., Trajectory hunting: Analysis of rapid chlorine activation in December 1992 as seen by UARS, *J. Geophys. Res.*, *105*, 4003–4018, 2000.

Danilin, M. Y., et al., Comparison of ER-2 aircraft and POAM-III, MLS, and SAGE-II satellite measurements during SOLVE using traditional correlative analysis and trajectory hunting technique, *J. Geophys. Res.*, *107*, doi:10.1029/2001JD000781, in press, 2002.

Deniel, C., et al., A comparative study of POAM-II and ECC ozonesonde measurements obtained over northern Europe, *J. Geophys. Res.*, *102*, 23,629–23,642, 1997.

Froidevaux, L., et al., Validation of UARS MLS ozone measurements, *J. Geophys. Res.*, *101*, 10,017–10,060, 1996.

Gille, J. C., and L. V. Lyjak, Radiative heating and cooling rates in the middle atmosphere, *J. Atmos. Sci.*, *43*, 2215–2229, 1986.

Glaccum, W., et al., The Polar Ozone and Aerosol Measurement (POAM) instrument, *J. Geophys. Res.*, *101*, 14,479–14,787, 1996.

Gordley, L. L., et al., Validation of NO and NO_2 measurements made by the HALOE for UARS platform, *J. Geophys. Res.*, *101*, 10,241–10,266, 1996.

Harries, J. E., et al., Validation of measurements of water vapor from the HALOE, *J. Geophys. Res.*, *101*, 10,205–10,216, 1996.

Irie, H., et al., Validation of NO_2 and HNO_3 measurements from the Improved Limb Atmospheric Spectrometer (ILAS) with the version 5.20 retrieval algorithm, *J. Geophys. Res.*, *107*, doi:10.1029/2001JD001304, in press, 2002.

Kanzawa, H., et al., Validation and data characteristics of water vapor profiles observed by the Improved Limb Atmospheric Spectrometer

(ILAS) and processed with version 5.20 algorithm, *J. Geophys. Res.*, *107*, 10.29/2001JD000881, in press, 2002.
Kawa, S. R., et al., Interpretation of NO_x/NO_y observations from AASE-II using a model of chemistry along trajectories, *Geophys. Res. Lett.*, *20*, 2507–2510, 1993.
Koike, M., et al., A comparison of Arctic HNO_3 profiles measured by ILAS and balloon-borne sensors, *J. Geophys. Res.*, *105*, 6761–6771, 2000.
Lahoz, W. A., et al., Validation of UARS MLS 183 GHz H_2O measurements, *J. Geophys. Res. Lett.*, *101*, 10,129–10,150, 1996.
Lu, J., V. A. Mohnen, G. K. Yue, R. J. Atkinson, and W. A. Matthews, Intercomparison of stratospheric ozone profiles obtained by SAGE II, HALOE, and ozonesondes, *J. Geophys. Res.*, *102*, 16,137–16,134, 1997.
Lu, C.-H., G. K. Yue, G. L. Manney, H. Jäger, and V. A. Mohnen, Lagrangian approach for SAGE II profile intercomparisons, *J. Geophys. Res.*, *105*, 4563–4572, 2000.
Manney, G. L., et al., Polar vortex dynamics during spring and fall diagnosed using trace gas observations from the ATMOS instrument, *J. Geophys. Res.*, *104*, 18,841–18,866, 1999.
Manney, G. L., et al., Comparison of satellite ozone observations in coincident air masses in early November 1994, *J. Geophys. Res.*, *106*, 9923–9944, 2001.
Massie, S. T., et al., Chlorine activation during the early 1995–1996 Arctic winter, *J. Geophys. Res.*, *105*, 7111–7131, 2000.
Michelsen, H. A., G. L. Manney, M. R. Gunson, and R. Zander, Correlations of stratospheric abundances of NO_y, O_3, N_2O, and CH_4 derived from ATMOS measurements, *J. Geophys. Res.*, *103*, 28,343–28,359, 1998.
Morris, G. M., et al., Trajectory mapping and applications to data from the UARS, *J. Geophys. Res.*, *100*, 16,497–16,506, 1995.
Morris, G. M., J. F. Gleason, J. Ziemke, and M. R. Schoeberl, Trajectory mapping: A tool for validation of trace gas observations, *J. Geophys. Res.*, *105*, 17,875–17,894, 2000.
Muscari, G., R. Dezafra, and M. L. Santee, Intercomparison of stratospheric HNO_3 measurements over Antarctica: Ground-based Millimeter-wave versus UARS/MLS version 5 retrievals, *J. Geophys. Res.*, *107*, doi:10.1029/2002JD002546, in press, 2002.
Park, J. H., et al., Validation of HALOE CH_4 measurements from the UARS, *J. Geophys. Res.*, *101*, 10,183–10,203, 1996.
Pierce, R. B., W. L. Grose, and J. M. Russell III, Evolution of southern hemisphere air masses observed by HALOE, *Geophys. Res. Lett.*, *21*, 213–216, 1994.
Pierce, R. B., et al., Photochemical calculations along air mass trajectories during ASHOE/MAESA, *J. Geophys. Res.*, *102*, 13,153–13,168, 1997.
Prather, M. J., and A. H. Jaffe, Global impact of the Antarctic ozone hole: Chemical propagation, *J. Geophys. Res.*, *95*, 3473–3492, 1990.
Press, W. H., et al., *Numerical Recipes: The Art of Scientific Computing*, Cambridge Univ. Press, New York, 1986.
Randall, C. E., D. W. Rusch, R. M. Bevilacqua, K. W. Hoppel, and J. D. Lumpe, Polar Ozone and Aerosol Measurement (POAM) II NO_2, 1993–1996, *J. Geophys. Res.*, *103*, 28,361–28,371, 1998.
Rex, M., et al., In situ measurements of stratospheric ozone depletion rates in the Arctic winter 1991/1992: A Lagrangian approach, *J. Geophys. Res.*, *103*, 5843–5853, 1998.
Rusch, D. W., et al., Validation of POAM-II ozone measurements with coincident MLS, HALOE, and SAGE-II observations, *J. Geophys. Res.*, *102*, 23,615–23,627, 1997.
Russell, P. B., and M. P. McCormick, SAGE-II aerosol data validation and initial data use, *J. Geophys. Res.*, *98*, 10,777–10,797, 1993.
Russell, J. M., III, et al., The halogen occultation experiment, *J. Geophys. Res.*, *98*, 10,777–10,797, 1993.
Salawitch, R. J., et al., The distribution of hydrogen, nitrogen, and chlorine radicals in the lower stratosphere, *Geophys. Res. Lett.*, *21*, 2547–2550, 1994.
Santee, M. L., et al., Six years of UARS MLS HNO_3 observations: Seasonal, interhemispheric, and interannual variations in the lower stratosphere, *J. Geophys. Res.*, *104*, 8225–8246, 1999.
Santee, M. L., et al., HNO_3 measurements from MLS on the UARS and EOS CHEM Satellites, paper presented at Am. Meteorol. Soc., Meeting, Long Beach, Calif., 2000.
Sasano, Y., et al., Improved Limb Atmospheric Spectrometer (ILAS) for stratospheric ozone layer measurements by solar occultation technique, *Geophys. Res. Lett.*, *26*, 197–200, 1999a.
Sasano, Y., et al., Validation of ILAS version 3.10 ozone with ozonesondes measurements, *Geophys. Res. Lett.*, *26*, 831–834, 1999b.
Schoeberl, M. R., and L. Sparling, Trajectory modeling, in *Proceedings of the International School of Physics: Diagnostic Tools in Atmospheric Physics*, edited by G. Fiocco and G. Visconti, pp. 289–305, Elsevier Sci., New York, 1994.
Schoeberl, M. R., M. Luo, and J. E. Rosenfield, An analysis of the Antarctic HALOE trace gas observations, *J. Geophys. Res.*, *100*, 5159–5172, 1995.
Shepherd, T. G., J. N. Koshyk, and K. Ngan, On the nature of large-scale mixing in the stratosphere and mesosphere, *J. Geophys. Res.*, *105*, 12,433–12,446, 2000.
Smith, A. K., and L. V. Lyjak, An observational estimate of gravity wave drag from the momentum balance in the middle atmosphere, *J. Geophys. Res.*, *90*, 2233–2241, 1985.
Stratospheric Processes and their Role in Climate (SPARC), SPARC assessment of upper tropospheric and stratospheric water vapour, *SPARC Rep. 2*, edited by D. Kley et al., 312 pp., Dec. 2000.
Sugita, T., et al., Validation of ozone measurements from the Improved Limb Atmospheric Spectrometer (ILAS), *J. Geophys. Res.*, *107*, 10.1029/2001JD000602, in press, 2002.
Sutton, R. T., et al., High-resolution stratospheric tracer fields estimated from satellite observations using Lagrangian trajectory calculations, *J. Atmos. Sci.*, *51*, 2995–3005, 1994.
Suzuki, M., et al., ILAS, the Improved Limb Atmospheric Spectrometer, on the Advanced Earth Observing Satellite, *IEICE Trans. Commun.*, *E78-B*, 1560–1570, 1995.
Swinbank, R., and A. O'Neill, A stratosphere-troposphere data assimilation system, *Mon. Weather Rev.*, *122*, 686–702, 1994.
Toon, G., et al., Comparison of ILAS and MkIV profiles of atmospheric trace gases measured above Alaska in May 1997, *J. Geophys. Res.*, *107*, 10.1029/2001JD000640, in press, 2002.
von der Gathen, P., et al., Observational evidence for chemical ozone depletion over the Arctic in winter 1991–92, *Nature*, *375*, 131–134, 1995.
Waters, J. W., Microwave limb sounding, in *Atmospheric Remote Sensing by Microwave Radiometry*, edited by M. A. Janssen, pp. 383–496, John Wiley, New York, 1993.

R. M. Bevilacqua, Naval Research Laboratory, 4555 Overlook Ave., Washington, DC 20375, USA.
M. Y. Danilin, The Boeing Company, P.O. Box 3707 MC OR-RC, Seattle, WA 98124, USA.
L. Froidevaux, W. G. Read, and M. L. Santee, NASA JPL, Mail Stop 183-701, 4800 Oak Grove Drive, Pasadena, CA 91109, USA.
H. Irie and Y. Kondo, Research Center for Advanced Science and Technology, The University of Tokyo, 4-6-1 Komaba, Meguro-ku, Tokyo 153-8904, Japan.
M. K. W. Ko and C. J. Scott, AER, Inc., 131 Hartwell Ave., Lexington, MA 02421, USA. (danilin@aer.com)
L. V. Lyjak, ACD, NCAR, P.O. Box 3000, Boulder, CO 80303, USA.
J. M. Russell III, Center for Atmospheric Sciences, Hampton University, Hampton, VA 23668, USA.
Y. Sasano, National Institute for Environmental Studies, Tsukuba, Ibaraki, 305-0053, Japan.
J. M. Zawodny, NASA Langley Research Center, Mail Stop 475, Hampton, VA 23681-2199, USA.